UNDERGROUND EXPLOSION TRIALS AT RAUFOSS 1968: BLAST WAVE PROPAGATION FOLLOWING A DETONATION IN A TUNNEL SYSTEM

K. G. Schmidt

Norwegian Defence Research Establishment
Kjeller, Norway

20 October 1970

(1)

INTERN RAPPORT X-128

FORSVARETS FORSKNINGSINSTITUTT
Norwegian Defence Research Establishment
Postboks 25 - Kjeller
Norge

FFIX
Intern rapport X-128
Reference: Job 203/736
Date: October

UNDERGROUND EXPLOSION TRIALS AT RAUFOSS 1968 : BLAST WAVE PROPAGATION FOLLOWING A DETONATION IN A TUNNEL SYSTEM

by

K G Schmidt

Approved
Kjeller, 20 October 1970

T Krog
Superintendent

FORSVARETS FORSKNINGSINSTITUTT
Norwegian Defence Research Establishment
P O Box 25 - N - 2007 Kjeller
Norway

CONTENTS

UNDERGROUND EXPLOSION TRIALS AT RAUFOSS 1963 : BLAST WAVE PROPAGATION FOLLOWING A DETONATION IN A TUNNEL SYSTEM

SUMMARY

The purpose of the present work was to examine the blast wave pressure to be expected at the entrance of a neighbouring chamber in an underground ammunition storage site when all the explosives in a chamber detonate simultaneously.

Blast wave propagation and temperature distribution in a simple tunnel system following a detonation were observed for TNT charges from 100 to 5400 kg.

The blast wave pressure measurements were fairly successful whereas the temperature measurements were not.

The peak pressures measured after firing a shot at the inner end of the tunnel were considerably greater than the corresponding peak pressures measured after firing an equally sized charge in the chamber. This is due to the branch tunnel having an effect as a blast trap.

A theoretical model to predict the expected peak pressure in the transport tunnel is discussed for shots fired in the chamber. For a loading density of 200 kg TNT/m^3 an air shock wave is predicted to have an overpressure within a range from 55 bars to 80 bars. For a loading density of 100 kg TNT/m^3 the overpressure is expected to be within a range from 35 bars to 55 bars.

1 INTRODUCTION

Underground storage of ammunition presents safety problems which are substantially different from those connected with aboveground storage.

The purpose of the present trials was to examine several aspects of the safety of underground ammunition storage with a particular view to problems concerning the connected chamber type storage sites, which are almost exclusively used in Norway. The trials were a continuation of previous studies which have been described in various reports (Ref 1, 2, 3, 4).

The specific objectives of the present trials were:

- to measure the blast wave and the temperature distribution in a tunnel when a detonation occurs in an adjoining chamber
- to consider the blast waves in view of a theory which is described elsewhere in this report
- to test a blast door and some other equipment against the blast and the ground shock from a detonation
- to measure peak pressures and pressure-time histories in the blast wave outside the tunnel
- to study the amount and distribution of debris ejected from the tunnel exit

Several of the tests and measurements have been reported elsewhere (See Ref 5, 6, 7, 8).

2 BACKGROUND INFORMATION AND THEORY

2.1 Expected general behaviour

Some theoretical calculations have been made in Ref 3 and 9 concerning the equilibrium pressure and temperature expected in a closed storage chamber when all the explosives detonate simultaneously. It was concluded that after a few milliseconds have elapsed to allow several shock reflections in the chamber, an equilibrium pressure of about 1070 bars and a temperature of 2500 ^{o}K would be attained for a loading density of 100 kg TNT/m^3.

In Ref 1 it was concluded that a detonation in a chamber with a loading density of 100 kg TNT/m^3 will cause a shock wave of about 100 bars at the entrance to the neighbouring chambers. If the loading density is increased to 200 kg TNT/m^3 it was concluded that the air shock wave will have a strength of about 120 bars at the entrance to the next chamber

It was further expected that the air shock will be followed by the explosive gases at a temperature between 1000 ^{o}K and 1500 ^{o}K. The duration of the pressure profile would be of the order of one second, while the temperature duration would be many seconds.

2.2 Previous experiments in underground tunnel systems and theoretical considerations

Several calculations and experiments concerning shock propagation in straight tunnels and shock tubes have been published in the recent years. However, most of this work differs from the present study in several ways: less-than-full-size smooth walled tubes with a simple geometry are considered, and the absence of explosive gases is assumed. A theory that would account for the complex initial and boundary conditions, all possible reflections and diffractions of the blast wave, and the energy fluctuations caused by the shifting chemical equilibria, would be quite unmanageable. Several simplifying assumptions have thus to be made.

An approach to the problem made by D R Curran and D Hveding has been presented in Ref 1. An exploding charge in a chamber will set up a very complex system of reflected and diffracted shock waves which propagate in different directions. The volume of the chamber and the mass of the explosive gases contained within it is assumed to be large compared with the mass of gas which passes through the outlet in the first short time period necessary for some reflections to take place in the chamber. The greatest pressure differences in the chamber are now expected to be approximately levelled out. The pressure in the chamber is then assumed to be of the same order as the equilibrium pressure which would have been obtained if the chamber was closed. This equilibrium pressure and temperature are calculated in Ref 9.

The model is based on the assumption that the chamber is closed by an imaginary membran. After several reflections have taken place, the membran is allowed to burst causing a shock wave to propagate into the air of the branch tunnel (See Figure 3.1) and a rarefaction wave to travel back into the explosive gases. The explosive gas front thus acts as a piston supporting an air shock in front of it. The air shock overpressure

is estimated by finding the intersection of the explosive gas adiabat and the Hugoniot curve of air.

In Ref 11 an information summary of blast patterns in tunnels and chambers is given. The data are mainly based on shock tube experiments in the family of shock tubes at Ballistic Research Laboratories. In Figure 2.1 a curve from Ref 11 is shown. This curve shows the incident shock overpressure versus the transmitted shock overpressure for a "T" junction in tunnels with equal cross section areas. The curve is supported by experiments up to about 10 bars and is accordingly an extrapolation for higher pressures. This curve predicts an appreciable reduction in the blast wave pressure.

In Ref 12 and 13 shock propagation through channels and ducts is studied. Some theoretical calculations based on simplifying assumptions and experimental values are presented. The pressure are, however, small and the particular kind of junction of interest for the present study is not included. Nevertheless, it is clearly demonstrated that a shock wave which propagates through a smooth channel with a cross section area increase, decreases in strength and vice versa.

Shock waves which propagate through a "T" junction will be assumed to decrease in strength according to Figure 2.1. If the shock waves in addition experience a cross section area increase, a greater decrease in the shock strength should actually be the result.

Workers at Ballistic Research Laboratories (Ref 10) have obtained data for the propagation of shock profiles in a variety of tunnel systems. Their data were taken from smooth walled tubes of diameters ranging from a few inches up to four feet. The attenuation of the peak pressure in a long straight and comparatively smooth tunnel was found to be described by the formula:

$$(P-1) = (P_i-1) \exp \left\{ -\left(\frac{\alpha}{D} + \frac{1}{T_i}\right) KX \right\} \qquad (2.1)$$

where P is the peak pressure in atmospheres a distance X from a point where the profile has a peak pressure of P_i atmospheres and a duration of T_i seconds. D is the tunnel diameter. K is given by

$$K = \frac{1}{S} - \frac{1}{U+C}$$

where S is the air shock velocity, U is the particle velocity behind the air shock front and C is the sound speed behind the air shock front. The parameter α is an experimentally determined parameter with dimensions of velocity. For smooth walls BRL found that $\alpha = (2.93\ P_i + 0.262)$ m/s, P_i is given in atmospheres.

The duration T_i is defined as shown in the sketch below and is determined by the slope of the pressure-time profile close to the peak pressure.

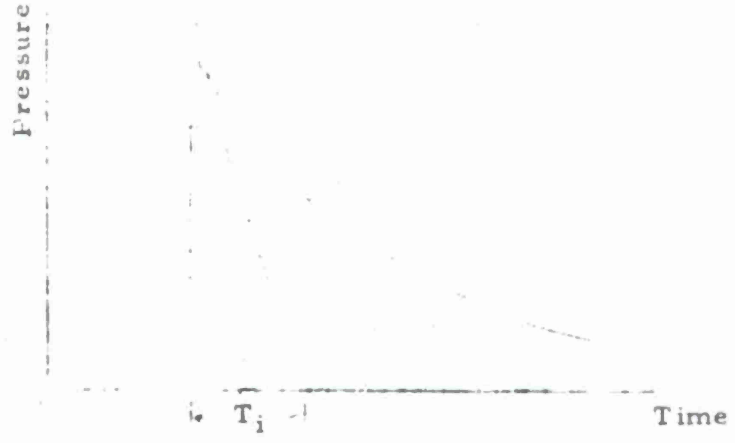

If the curve is exponential ($P = P_{max}\ e^{-t/\tau}$), then it can be shown that T_i is equal to the time constant τ.

In formula (2.1) it can be shown that the $\frac{KX}{T_i}$ term in the exponential is due to the overtaking rarefaction waves. The $\alpha \frac{KX}{D}$ term is an experimental term designed to account for all irreversible losses, which will be arbitrarily called "viscous" losses.

It can be seen that the form of Equation (2.1) is unfortunate in the case of low pressure, since in that case $K \rightarrow 0$, and the formula predicts no damping, whereas in fact we might still expect viscous losses. For high pressures, it can also be seen that $K \rightarrow 0$. This is not important, however, within the pressure region which is of interest here.

It should also be mentioned that in Equation (2.1) the term $\frac{1}{T_1}$ for long durations and for sufficiently high pressures can be small compared with the term $\frac{\alpha}{D} = \frac{2.93}{D} P_2 + \frac{0.262}{D}$. This is in accordance with the expected behaviour when "a flat" pressure pulse propagates through the tunnel. The attenuation is then more likely due to the "viscous" losses than to rarefaction waves overtaking from behind.

3 EXPERIMENTS

3.1 Object

The specific objectives of the trials to be described in the present report were to measure the blast waves and the temperature distributions in a tunnel when a detonation occurs in an adjoining chamber.

3.2 Description of experiments

3.2.1 Experimental procedure

The experimental procedure consisted in detonating explosive charges in a chamber. To achieve high-pressure loads on a blast door, reported in Ref (6), charges were also fired at the end of the tunnel.

3.2.2 Tunnel system

A short tunnel - 30 m long - existed before these trials were planned. This tunnel was lengthened and two side chambers connected to the tunnel were constructed as shown in Figure 3.1. The branch passageway had a cross section area of 2.4 m^2 whereas the transport tunnel was 5.5 m^2. The volume of the detonation chamber was 54 m^3. The tunnel system can very roughly be considered as a half scale model of a typical Norwegian underground storage site.

The walls and roofs in the two chambers were covered with gunite (sprayed concrete).

The blast door mentioned, was installed at the inlet of a measurement chamber.

The total detonation chamber overhead cover was about 13 m. It turned out, however, that the soil layer in this area was much deeper than expected so the thickness of rock was only 5 - 6 m. The strength of the rock was not very high due to several cracks which existed when the trials started, and which were observed to be extended after each shot in the chamber.

3.2.3 Measurement and recording instruments

The positions of the measurement stations (m st) numbered from 1 to 8 can be seen at Figure 3.1 and Figure 3.2. Six measurement stations numbered from 3 to 8 were situated in the roof while measurement station 2 was situated in the foundation beside the door. Measurement station 1 was installed in the chamber behind the door.

Each measurement station was equipped with a pressure time gauge and a thermocouple.

The thermocouples were Philips thermocoax 2 ABAc which could measure temperatures up to 1200 ^{o}C The response time of a thermocouple is a function of the particle velocity past the junction. The response time in milliseconds for these thermocouples increases from 200 to

Piezoelectric pressure time transducers were used for the pressure measurements. In the tunnel Kistler 701 H transducers were installed while a more sensitive Atlantic Research Corporation piezoelectric gauge LC 13 was mounted in the chamber behind the door (m st 1). The Kistler 701 H gauge had a sensitivity of 80 pc/at, a resonant frequency of 65 kHz, and could measure pressure up to about 600 bars. The I C 13 gauge had a sensitivity of 500 pc/psi and could measure pressure up to about 14 bars.

An installation in the roof is shown in Figure 3.3. The same instrument holder was used in measurement station 2. The cables from the gauges ran through drill holes to the surface. In the measurement chamber behind the door a different instrument holder bolted to a concrete platform was applied. The cables from measurement station 2 were led through a drill hole in the ceiling of the measurement chamber up to the surface.

The signals from the thermocouples were recorded by a CEC-galvanometer oscillograph. CEC 7 - 343 galvanometers were applied which had a flat frequency range of 0 - 200 Hz and a sensitivity of 0.165 in/mV.

The pressure gauges were connected to charge amplifiers with a frequency range of 0 - 150 kHz.

The recording instruments were Ampex FR 1300 tape recorders with a frequency response from 0 to 20 kHz.

The amplifiers were placed above the measurement chamber on a soft mat to avoid disturbances from the ground shock. The recording instruments were placed a distance of about 200 m from the amplifiers in a recording station.

3.2.4 Experimental difficulties

Disturbances caused by the ground shock are an inherent difficulty in underground trials. Noice caused by the ground shock was present at some pressure records. Usually it damped rapidly out before pressures were measured by the gauges.

The cable leading from measurement station 2 to its amplifier was in most cases affected by the ground shock during the trials and set into mechanical oscillations. The pressure time history recorded at this station is therefore less reliable. The pressure rise due to the arrival of the blast wave should, however, be negligibly affected.

Instrument holders as shown in Figure 3.3 were mounted in the roof to protect the gauges in the tunnel. As an undesired consequence, the fluid velocity past the junction was too low to provide sufficient response of the thermocouples.

3.3 Experimental results

3.3.1 Explosive charges fired

All charges consisted of cast TNT blocks. An outline of the shots fired is given in Table 3.1 below. The positions of the charges, the distance from each charge center to measurement station 3 ahead of the door, and the height above the floor can also be seen from the table.

Shot	Charge weight kg	Place	Distance to m st 3	Distance from charge center to floor
1	100	Tunnel	18.90 m	1.40 m
2	100	"	"	"
3	100	Chamber	21.15 m	"
4	301	"	21.20 m	1.00 m
5	298	"	"	"
6	294	Tunnel	18.90 m	"
7	999	Chamber	21.20 m	0.50 m
8	1003	Tunnel	21.85 m	0.75 m
9	1001	"	17.68 m	0.50 m
10	5426	Chamber	21.90 m	"

Table 3.1 Shots fired

The first six charges were placed on [illegible]

3.3.2 Calculated pressure based on the arrival times

The time for the blast wave to arrive at the respective measurement stations was measured. The number of measurements for each shot varied from 4 to 6. The data are presented in Table 3.2. A smooth curve was then fitted to the arrival time distance data by the method of least squares. A discussion of choice of curves and method of calculation is given in Ref (14). The shock arrival time versus distance from the charge obtained by curve fitting to the measured data can be seen in Figure 3.4 and Table 3.3. It should be mentioned that the time of trigger was lost for shot 4, 5 and 7. For these shots the arrival time at measurement station 3 was arbitrarily chosen as 20 ms. The curves were differentiated and the blast wave velocity obtained. The velocity and the appropriate Rankine-Hugoniot relation determine the blast wave pressure along the tunnel.

Pressure-distance curves could either be based on the distance from the charge or from a fixed point in the tunnel, for instance m st 3. Both type of curves, where pressure means the absolute pressure (shock overpressure plus atmospheric pressure), are presented in Figure 3.5 - 3.8.

3.3.3 Measured pressure

The pressure records from measurement stations 2 - 8 are presented in Figures 3.9 - 3.23. The pressures calculated from arrival time data are also shown on the records. It should be noted that the difference in the calculated pressure between measurement station 2 and 3 due to their position along the tunnel is small, and the calculated pressures for measurement station 3 are therefore also indicated at the records from measurement station 2. The pressure records presented, are traced from the original records and some loss in quality may therefore be expected.

The quality of the measurements was not constant for all shots. Drift in the zero adjustment can be seen on records from the first five shots. This difficulty was avoided for the later shots. The precision of the

measurement chain was estimated to about 10 %. The initial values of the pressure curves are thus expected to be of a similar precision. The precision of the pressure-time history is also expected to be quite good when the zero adjustment of the amplifiers is proper. The precision at later stages of the pressure records may, however, be slightly reduced due to heat exchange from the explosive gases to the gauges. In view of the uncertainty in the interpretation of the pressure curves, the precision is considered to be sufficient.

The pressure-time history recorded from measurement station 2 was generally of poorer quality than the pressure measurements at other stations. This was due to vibrations in the cable leading to the gauge. Several attempts to prevent this were not successful. The records from measurement station 2 are presented, however, because the rapid rise in pressure due to the arrival of the shock front is assumed to be relatively unaffected by the induced disturbance in the cable.

The pressure records from shot 10 differ from records from the previous shots. The overhead cover of the detonation chamber was not of good quality and sufficient thick to contain the effects of this shot, and a crater was formed. As a consequence the pressure-time history in the tunnel was highly affected by a decrease in the duration. The "piston" effect supporting the shock propagation will be weaker than in a contained detonation. Accordingly the attenuation of the blast wave will increase more with distance along the tunnel in this case. Another effect from the blow-through was that the amplifiers and cables at the surface were exposed to considerable disturbances by moving rock from the crater which broke cables and burried the amplifiers. Nevertheless, as a crater formation takes some time, the pressure-time history recorded at m st 2 and 3 within the first 10 milliseconds is likely to be unaffected by the formation of a crater.

3.3.4 Discussion of pressure records

Pressure records from pressure measurements in the open are often approximated by exponential curves. Pressure curves from measure-

ments of the shock wave propagation in smooth pipes and in shock tubes may also frequently exhibit exponential shape. The pressure records presented here differ in some respects from exponential shape. They start with the ordinary steep rise at the initial stage due to the shock front, immediately followed by some high and narrow spikes behind which broader spikes take place before the curve starts to smooth out as the overpressure decreases.

In previous experiments in underground tunnel systems (Ref 1) the pressure-time elapse was observed to be somewhat different from what is observed here. A low pressure precursor followed by several peaks of higher pressure was measured, and the shock velocity usually was in agreement with the low pressure precursor. It was thought that the low pressure precursor was due to the spherically expanding part of the original blast wave, which at the moment was not overtaken by the higher pressure waves which were built up from behind through the process of multiple reflections from the walls.

According to this conception it follows from the initial parts of the pressure curves, Figures 3.9 - 3.23, that the measurement stations have been at sufficient distance from the charges to let the higher pressure waves due to multiple reflections, overtake the expanding part of the original blast wave.

It is then likely that the blast wave following a detonation in the tunnel system consists of a relatively plane shock wave moving along the tunnel axis, superposed by a great number of waves generated by the process of multiple reflections and diffractions with the irregular walls in the tunnel. The calculated pressure based on the arrival times should then approximate the plane shock wave component, which may frequently have a lower value than the total peak overpressure felt by the gauge.

Local geometrical irregularities may also be responsible for some of the anomalies of the pressure records. As an example consider measurement station 3. Figures 3.2 and 3.24 show the position of the station. During the excavation of the measurement chamber a mass of heavy rock in the roof ahead of the chamber inlet fell down. To mount

the station at the level of the roof profile a protruding concrete foundation was made. No calculation can be made to show the influence of this to the records. But the records from this station exhibit stronger oscillations at the initial stages than records from other stations in the roof. The records from this station also exhibit higher peak pressures than records from measurement station 2.

The measured peak pressure is according to the previous discussion expected to be equal to or greater than the calculated pressure (derived from arrival time data). The maximum side-on pressure in the blast wave should generally be bounded by the calculated pressure and the peak pressure felt by the gauge. When an appreciable difference exists between the measured peak pressure and the calculated pressure, the side-on pressure in the blast wave may be approximated by smoothening the pressure curves to for example an exponential shape by conserving the area under the curve.

Accordingly the pressure curves presented here will be interpreted in the following ways:

1) The maximum pressure can be taken directly from each curve when some care is taken to avoid spikes which do not contain an appreciable area. Such spikes could possibly be due to local disturbances near the gauge and to noice in the measurement chain.

2) The curves can be smoothened to an exponential shape so that the areas under the curves are approximately conserved.

The blast waves from detonations in the chamber were of main importance for the purpose of this report. Some shots were, however, fired at the end of the tunnel particularly to expose a blast door to high pressure blast wave loads (Ref 6). These shots are also included in Table 3.1. A look at the figures containing the calculated pressure (Figures 3.5 - 3.8) and the pressure records (Figures 3.9 - 3.23) demonstrates that the measured pressures from shots of equal charge size fired in the chamber and in the tunnel are different.

At m st 3 the peak pressure of the blast wave following a charge fired at the end of the tunnel is considerably greater than the blast wave following a similar charge fired in the chamber. This difference seems to increase with the charge size.

Blast waves from charges fired at the end of the tunnel tend to be of shorter duration compared with similar shots in the chamber as the pressure records exhibit a more rapid decay with time. Pressure-time histories from tunnel detonations also tend to have smoother pressure profiles than the pressure profiles following chamber detonations. This is frequently the case for pressure records from m st 3.

Interesting differences are observed when we compare the pressure data from shots 8 and 9. The charge fired as shot 8 was arranged in a stack close to the end wall of the tunnel, Figure 3.25. This shot resulted in several cracks in the tunnel walls and the roof near to the charge. For safety reasons the following shot was fired about 4.2 m from the end of the tunnel (Table 3.1).

The difference in peak pressure is considerable in this case as displayed for example on Figures 3.6 and 3.8. The attenuation differs also between the two shots as the blast wave propagates through the tunnel. The peak pressure in the blast wave following shot 8 is much greater than the corresponding pressure following shot 9. The peak pressure in the blast wave following shot 8 attenuates stronger than what is the case after firing shot 9, and it decreases below the corresponding peak pressure in the blast wave of the following shot near the end of the tunnel.

3.3.5 Pressure duration

Both the definition and measurement of the pressure duration introduce difficulties. Some of the pressure-time profiles measured here can approximately be considered to have triangular shape. Frequently, however, it is better to approximate the pressure curves by an exponential curve at the initial stage. It follows that the term duration would mean something quite different in these two cases.

Consequently, the term duration must be defined to be meaningful. But the duration according to a definition can not be found independently of how the pressure curve is read and the side-on pressure assigned to the blast wave is derived.

Accordingly any set of values of a duration will contain great uncertainties. A set of such data will further not provide any measure of time in which appreciable pressure can be measured. The term duration is not particularly useful, and it is thus hard to find support to present a set of such data from the pressure records.

3.3.6 Temperature measurements

As mentioned elsewhere, the thermogauges at each measurement station in the roof were located in an installation which is shown in Figure 3.3.

The installation provided necessary protection of the gauge from the blast waves. As an undesired consequence, the fluid velocity past the junction was too low to provide sufficient sensitivity of the gauge. Temperature deflection was recorded at the galvanometer oscillograph, but the maximum temperature measured was far too low, and no correction can be given. The temperature measurements were thus unsuccessful. The temperature records following shot 7 are as an example shown in Figure 3.27.

4 COMPARISON OF THEORY AND EXPERIMENTS

4.1 Tentative correction of the BRL data

The exponent in Eq 2.1 contains the factor $\alpha = (2.93\ P_2 + 0.262)$ m/s which was experimentally determined in smooth walled tubes.

The experimental constants in the expression for α, Eq 2.1 will here be tentatively adjusted according to the present condition with rough walls etc. The value of α obtained that way will then be applied to the model previously described to predict the pressure in similar tunnel systems.

The experiments of the present trials differed from those of BRL in two important respects:

1) The presence of hot explosive gases in the tunnel

2) The roughness of the tunnel walls

As stated earlier the term containing α was designed to take account of all the irreversible losses. Accordingly it is expected that the experimentally determined constants contained in α would have been different if the walls in the shock tubes had been rough. The constant multiplied by P_2 in the expression for α contributes more to α than the additive constant does even for moderate pressures, so the latter will be neglected here.

It was previously discussed why the pressure duration was difficult to account for. A definition of the pressure duration, as the time for the pressure to drop to 1/e of the maximum value, applied to these curves might result in values in the range of 20 - 100 ms. An inspection of the exponent in Eq 2.1 shows that the term containing α may particularly for blast waves of higher pressure and long duration in a tunnel with rough walls, dominate the term containing $1/T_i$. It is therefore worthwhile to see if the pressure data can provide support to this assumption.

P_1 and P_2 represent the calculated pressure at measurements station 3 and 7 respectively, in Table 4.1 below. The peak pressures from the records according to interpretation 2 might in principle as well have been chosen. The peak pressure is, however, not as well defined as the calculated pressure. This is unfortunate as the term $(\frac{\alpha}{D} + 1/T_1)$ appears to be sensitive, when it is calculated, to uncertainties in the pressure data. S_1 and S_2 in the table are the distances respectively, from the charge to measurement station 3 and 7.

Shot	P_1	S_1	P_2	S_2	$\frac{\alpha}{D}+\frac{1}{T_1}$	$\frac{\alpha}{P_1}$
	bars	m	bars	m	s^{-1}	$\frac{m}{s\ bar}$
10 C	21.1	21.90	8.0	60.65	176	22
7 C	6.4	21.20	3.7	59.95	64	26
4-5 C	4.6	21.20	2.9	59.95	50	29
3 C	4.4	21.09	2.1	59.74	91	55
9 T	24.2	17.60	8.3	56.35	207	23
8 T	34.0	21.85	8.0	60.60	332	26
6 T	15.1	18.90	5.3	57.65	170	30
2 T	6.8	18.90	4.1	57.65	62	21

D = 2.65 m

Table 4.1 Tentative correction to the "viscous" term in the BRL formula

The calculation of $\left(\frac{\alpha}{D}+\frac{1}{T_i}\right)$ is based on Eq 2.1 and data presented in the table. When it is assumed that $\frac{1}{T_i}$ can be ignored relative to $\frac{\alpha}{D}$, the ratio $\frac{\alpha}{P_1}$ can be calculated and incorporated in the table.

An inspection of Table 4.1 shows that the ratio $\frac{\alpha}{P_1}$ is in the range of 20 - 30 for the 300 kg, 1900 kg and 5400 kg shots which provides some support to the assumption. If durations in the range of 3 - 35 ms are assumed with shorter duration to higher pressures, a significant decrease in the values of $\frac{\alpha}{P_1}$, presented in the table is attained. A greater number of measurements and shots than attained in these trials is necessary, however, to verify these ideas. Nevertheless, if we ignore the term $\frac{1}{T_i}$ and apply as an effective value $\frac{\alpha}{P_1} = 20$ for shots fired in the chamber, a conservative estimate of the attenuation would be the result for higher pressures.

4.2 Data obtained from the theoretical model

The detonation chamber is assumed to be closed and its initial pressure depending on the charge density is calculated by the methods of Ref (9). The results are presented in Table 4.2 (page 28) for actual shots and charge densities.

The air shock which propagates into the branch tunnel is then calculated by finding the intersection between the gas adiabat for the explosive gas and the Hugoniot curve of air for each shot.

This is done for $\gamma = 1.3$ and $\gamma = 1.5$. The first value of γ is to be applied for moderate pressures while $\gamma = 1.5$ is supposed to be an effective value of γ to account for real gas effects at higher pressures and temperatures. The results are presented in the table.

The shocks which propagate down the 5 m long branch tunnel are assumed to attenuate according to the BRL formula with an effective value of $\frac{\alpha}{p_1} \sim 20$ thus providing a conservative estimate of the attenuation. Values for the blast wave peak pressure at the outlet of the branch tunnel estimated by this method are also presented in Table 4.2.

These data are finally applied to the extrapolated data of Ref (11) which are presented in Figure 2.1. The results can be seen in the table for both values of γ together with the measured peak pressure from measurement station 3 which was the station situated nearest the junction.

4.3 Discussion

The theoretical model presupposes that the chamber is closed by an imaginary membran until equilibrium pressure is attained. For a loading density of 100 kg TNT/m^3 the equilibrium pressure is estimated to 1070 bars. As a comparison we will consider the blast wave from a centrally located detonating charge in a spherical chamber as the blast wave reaches the chamber wall. For the same loading density the leading blast pressure at this distance is 250 bars. This shows that the wave front has a much lower pressure than the gases behind which have a maximum pressure probably well above 1070 bars. It is then also clear that a classical shock front with both a uniform decaying pressure-time history and a uniform decaying pressure-distance distribution is not yet formed at this stage. The comparison indicates, however, that the model is a fair approximation of the actual phenomena.

The use of the extrapolated curve in Figure 2.1 represents some uncertainty. More important is probably the fact that the cross section area of the transport tunnel is twice the size of the branch tunnel. The attenuation of the blast wave in the "T" junction seems therefore to be underestimated.

Some attenuation of the blast wave will also occur during its travel from the junction to measurement station 3, which represents a distance of 11 m.

A disturbing factor is the reflection of the blast wave at the end of the transport tunnel, which would increase the peak pressure of the actual wave compared to that of the model. It does not seem likely, however, that this effect is appreciable at such a short range as the distance from the junction to measurement station 3.

Table 4.2 shows a fair agreement between the measured peak pressures according to interpretation 1 and those obtained by the model using $\gamma = 1.5$. It may therefore be expected that the model could also be used with some confidence at higher loading densities where experimental data are lacking. This has been done in Table 4.2 for the loading densities 200 and 270 kg/m^3.

It is obvious, however, that considerable uncertainties are involved in the methods used for the theoretical calculation. Also the experimental data should be regarded with some suspicion, particularly at the shortest distances, where unpredictable reflections and refractions may cause a very irregular propagation of the blast wave with great local variations of the blast pressure. Previous trials (Ref 1) indicated higher pressures than those reported here. Even if the present results are thought to be more reliable due to an improved measurement technique, it is nevertheless felt that some consideration should be given to the previous results. It is therefore suggested that the present values of the side-on pressures should be multiplied by a factor of 1.5 to obtain an estimate of the upper limit of the shock strength for the various loading densities.

The model exhibits some properties which should be noted.

The blast wave attenuates while it propagates through the branch tunnel. This can be seen from Table 4.2 for both values of γ. Table 4.2 also reveals that the attenuation increases with pressure. Eq. 2.1 shows that the pressure attenuation also increases with increasing length and reciprocal diameter of the branch tunnel. Rough walls contribute in the same direction. The numbers in the paranthesis indicate as an example what to be expected when the cross-section area of the branch tunnel is 5 m^2.

Further attenuation takes place as the blast wave propagates through the junction connecting the branch tunnel and the transport tunnel. The data presented in Figure 2.1 are given for tunnels of equal cross-section areas. An increase in the ratio between the cross-section area of the transport and the branch tunnel would provide a greater pressure decrease than indicated by the data of Figure 2.1. For the test site this ratio is 2. For an actual underground storage site a greater ratio might be favoured.

Table 4.2 shows the total effect of these phenomena as estimated by the model.

For a loading density of 100 kg TNT/m^3 we can see that the pressure undergoes a total decrease of about 50 % while it propagates through the branch tunnel and the junction into the transport tunnel. This demonstrates that this connection between the chamber and the transport tunnel constitutes an effective blast trap.

5 CONCLUSION

5.1 Expected effects in a tunnel outside neighbouring chambers in the event of a mass detonation in a storage chamber

In the full scale case and with a loading density of 200 kg TNT/m^3 it is concluded that the air shock will probably be within the range

55 - 80 bars. If the loading density is reduced to 100 kg TNT/m^3 the air shock overpressure at the entrance to the next chamber is expected to be within a range of 35 - 55 bars.

The air shock wave will pass the entrance to a neighbouring chamber about 15 - 25 ms after the detonation. The explosive gases follow behind the air shock at temperature expected to be above 1000 ^{o}K.

Blast waves following shots fired at the end of the tunnel may within about 10 tunnel diameters from the charge have a peak pressure of 3 to 5 times the peak pressure in blast waves from corresponding charge sizes fired in the chamber.

The peak pressure in the blast wave following a detonation of a 1000 kg TNT charge located close to the end of the tunnel is demonstrated to be considerably higher than the peak pressure in the blast wave following a detonation of a similar charge placed a few tunnel diameters from the tunnel's end. The attenuation of the first mentioned blast wave is, however, greater in this case so the peak pressure of this blast wave may with increasing distance decay to a value below the peak pressure of the latter at corresponding places in the tunnel.

The term duration is not thought to be particularly useful to blast waves in tunnel systems. For a full scale detonation, however, the time in which an appreciable pressure is measured, is in the order of 1 second.

Installation of blast doors, as described in Ref (6), at the entrance to the storage chambers in underground ammunitions storage sites similar to the test site, will probably provide effective protection against the air shock and the explosive gases to the chambers behind for loading densities higher than 100 kg TNT/m^3.

References

(1) Curran, D R - Underground storage of ammunition Experiments concerning accidental detonation in an underground chamber, Intern rapport X-111, Norwegian Defence Reasearch Establishment (1966)

(2) Løken, P C - Calculation and observation of the ground shock from underground detonations in rock, Intern rapport X-112, Norwegian Defence Research Establishment (1966)

(3) Curran, D R - Effects of an underground explosion in an underground chamber, Teknisk notat X-132, Norwegian Defence Research Establishment (1965)

(4) Curran, D R - Test of a blast door's response to blast waves and ground shocks, Intern rapport X-116, Norwegian Defence Research Establishment (1967)

(5) Strømsøe, E - Detonation trials in a tunnel system Preliminary report, Intern rapport X-122, Norwegian Defence Research Establishment (1969)

(6) Schmidt, K G - Underground Explosion Trials at Raufoss 1968. Test of a blast door's response to blast waves, Intern rapport X-125, Norwegian Defence Research Establishment (1970)

(7) Strømsøe, E - Underground explosion trials at Raufoss 1968. Measurement of air blast outside the tunnel, Intern rapport X-124, Norwegian Defence Research Establishment (1969)

(8) Aarak, S - Registrering av stenutkast ved sprengning i tunnel, Teknisk notat X-209, Norwegian Defence Research Establishment (1969) (In Norwegian only)

(9) Strømsøe, E - Estimate of the post detonation pressure and temperature of TNT charges in a closed chamber, Teknisk notat X-222, Norwegian Defence Research Establishment (1969)

(10) - Symposium Proceedings : Operation Snow Ball, Volume 1 August 1965 DASA 1642-1

(11) - Information Summary of Blast Patterns in Tunnels and Chambers, 2nd Edition, DASA Report No 1273

(12) Schardin, H
Reichenbach, H - Verhalten von Stosswellen in Kanalen und beim Eindringen in Eingangsbauwerke, Bericht Nr 8/65, Ernst Mach Institut, Freiburg i. Br

(13) Reichenbach, H - Stosswellenausbreitung in Kanalen mit abwinkelungen und abzweigungen, Bericht Nr 9/65, Ernst Mach Institut Freiburg i. Br

(14) Strøm.søe, E - Air shock o erpressure derived from arrival time data in an underground explosion, Teknisk notat X-187, Norwegian Defence Research Establishment (1967)

Shot 2		Shot 3		Shot 4 and 5		Shot 6	
Dist m	Time ms	Dist m	Time ms	Dist m	Time ms	Dist m	Time ms
18.90	16.5	21.15	21.1	21.20	20.0	18.90	15.6
21.10	29.5	31.35	38.0	31.40	35.3	29.10	24.0
39.10	43.0	59.90	93.4	41.40	52.1	39.10	36.8
49.10	57.6	80.42	140.0	51.40	69.1	49.10	47.0
				59.95	84.5	57.65	57.5
						78.17	90.5

Shot 7		Shot 8		Shot 9		Shot 10	
Dist m	Time ms	Dist m	Time ms	Dist m	Time ms	Dist m	Time ms
21.20	20.0	21.85	15.5	17.60	11.6	21.90	18.9
31.40	32.0	32.05	22.3	37.80	27.8	42.10	36.5
41.40	48.0	42.05	30.2	47.80	36.0	52.10	44.5
51.40	62.7	52.05	38.5	56.35	45.5	60.65	54.0
59.95	75.8	60.60	47.4	76.87	71.0	81.17	80.6
		81.12	75.0				

Table 3.2 Measured arrival time distance data

Shot	2	3	4 and 5	6	7	8	9	10
Distance m	Time ms	Time ms	Time ms	Time ms	Time ms	Time ms	Time ms	Time ms
20.00	17.86	19.46	18.14	16.44	18.13	14.65	13.27	17.71
30.00	30.63	35.45	33.34	25.59	31.12	20.62	20.63	25.07
40.00	44.33	53.42	49.52	36.26	45.18	28.01	29.15	33.52
50.00	58.92	73.03	66.63	48.42	60.25	36.93	38.86	43.11
60.00	74.35	93.96	84.58	62.01	76.26	47.40	49.76	53.83
70.00	90.57	115.95	103.30	76.93	93.16	59.41	61.84	65.68
80.00	107.53	138.83	122.71	93.09	110.86	72.90	75.06	78.63
St. deviation	0.38	0.13	0.1	0.81	0.50	0.50	0.48	0.74

Function used for curve fitting : $S/C - T = A_o + A_1 \text{ Ln } (T+T_o)$

S = distance, T = time, C = sound velocity at 7 °C, A_o, A_1 and T_o are constants to be determined for each fitting

Table 3.3 Arrival time distance data obtained by curve fitting to the measured data of Table 3.2

Shot	Charge weight	Charge density	Initial pressure chamber	MODEL $\gamma = 1.3$ Peak pressure at inlet of branch tunnel	outlet of branch tunnel	transport tunnel	$\gamma = 1.5$ Peak pressure at inlet of branch tunnel	outlet of branch tunnel	transport tunnel	Measured peak pressure according to interpret I	according to interpret II	calculated pressure
	kg	kg/m^3	bars	bars	bars	bars	bars	bars	bars	bars	bars	bars
3	100	2	29	10	9	6	10	9	6	5.5	3.2	3.4
4	300	7	62	16	14	10	15	13	9	7.6	6.4	3.6
5	300	7	62	16	14	10	15	13	9	8.1	5.3	3.6
7	1000	20	180	29	24(25)	17(16)	26	21(22)	15(16)	18	12.5	5.4
10	5100	100	1070	69	50(55)	36(40)	58	43(47)	31(34)	32		20.1
		200	2900	120	78(89)	56(64)	99	67(76)	49(54)			
		270	4200	144	90(103)	68(72)	117	76(87)	55(63)			

The cross-section area of the branch tunnel is 2.4 m^2. The numbers in the paranthesis indicate what to be expected if the cross-section area of the branch tunnel is 5 m^2

Table 4.2 Comparison of model with measurements

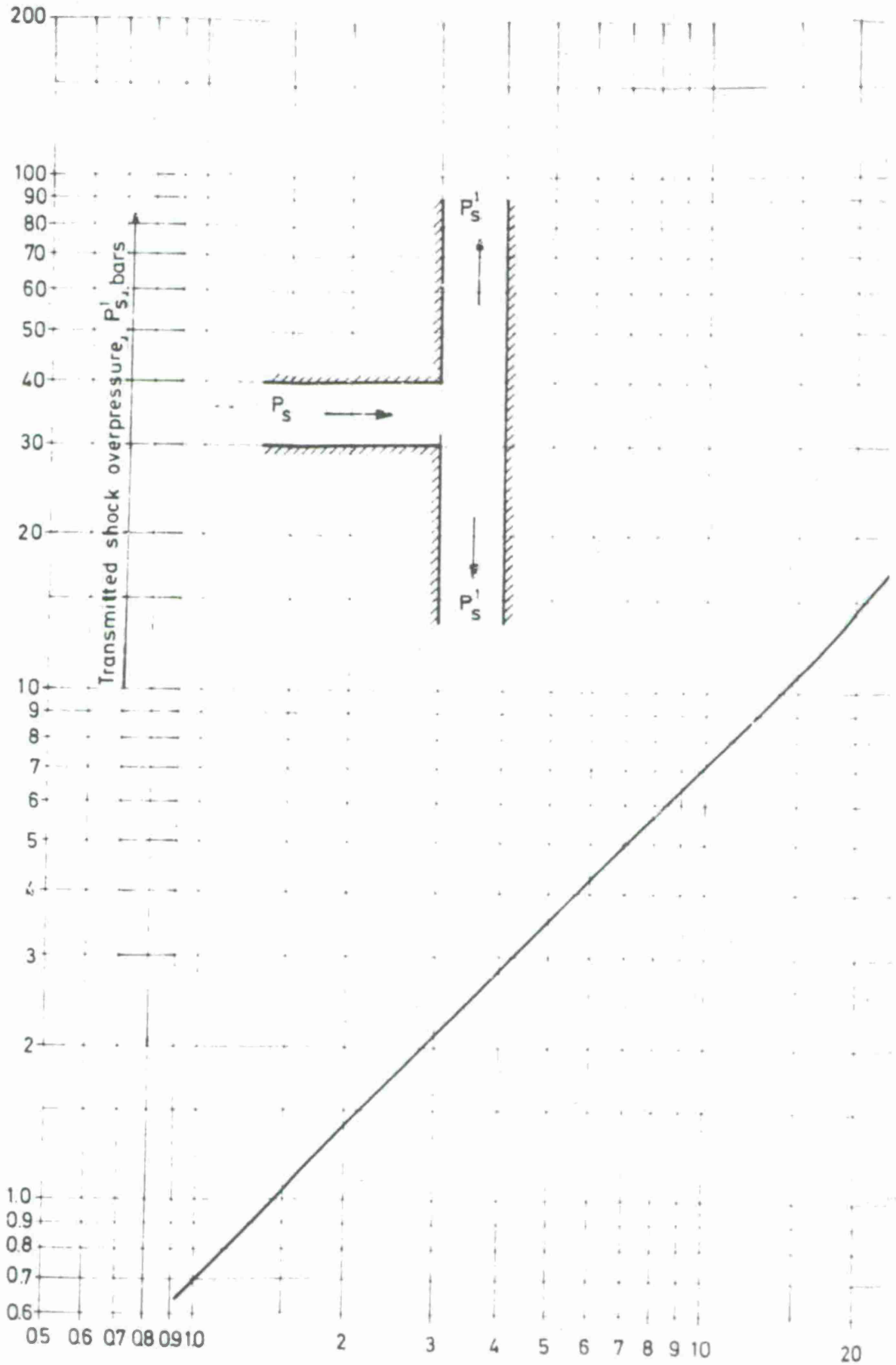
200
100
90
80
70
60
50
40
30
20
10
9
8
7
6
5
4
3
2
1.0
0.9
0.8
0.7
0.6
Transmitted shock overpressure, P'_s, bars
P_s
P'_s
P'_s
0.5 0.6 0.7 0.8 0.9 1.0
2
3
4
5
6
7
8
9
10
20

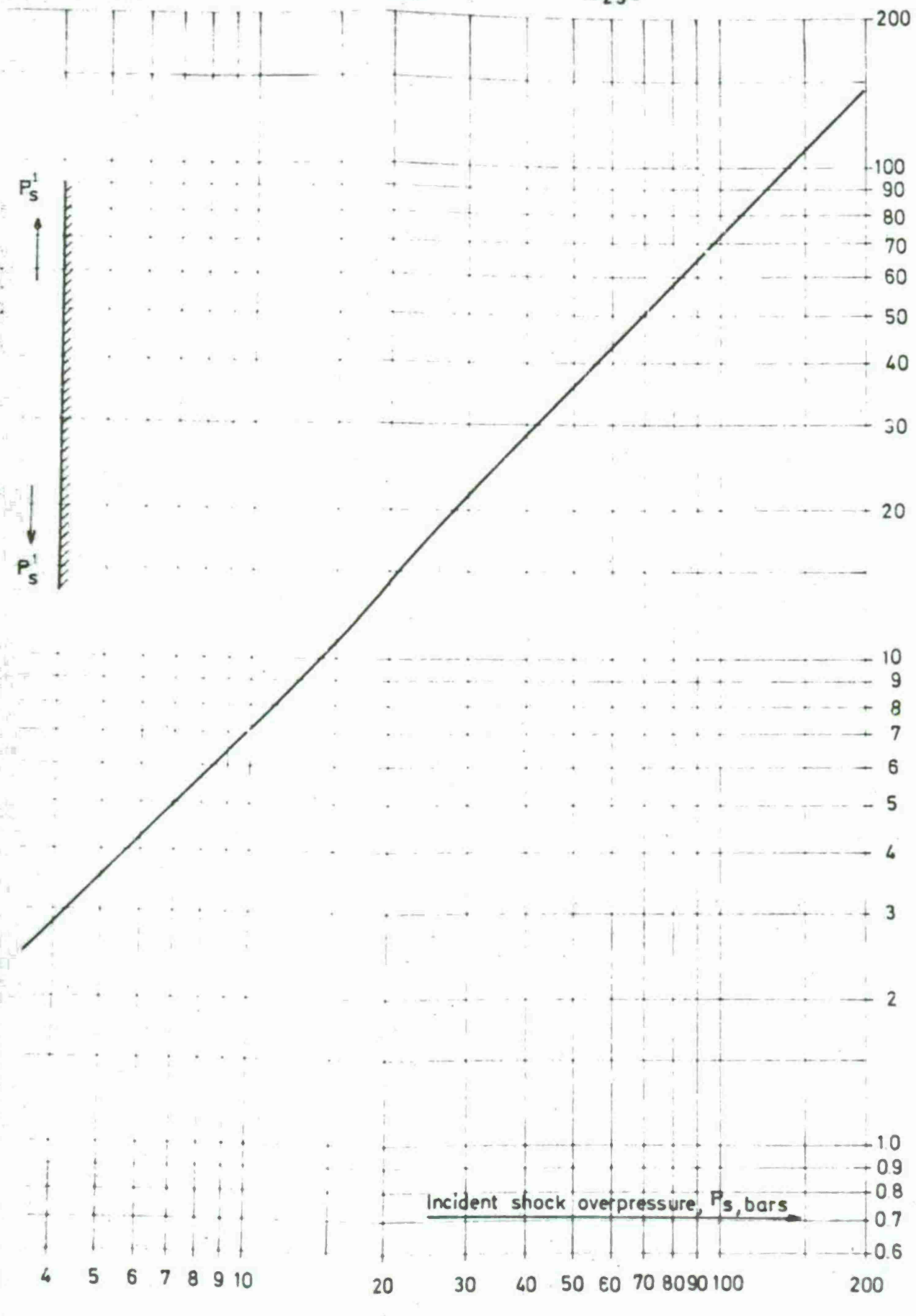
P_s^1
P_s^1
200
100
90
80
70
60
50
40
30
20
10
9
8
7
6
5
4
3
2
1.0
0.9
0.8
0.7
0.6
Incident shock overpressure, P_s, bars
4 5 6 7 8 9 10
20 30 40 50 60 70 80 90 100 200

Measurement stations

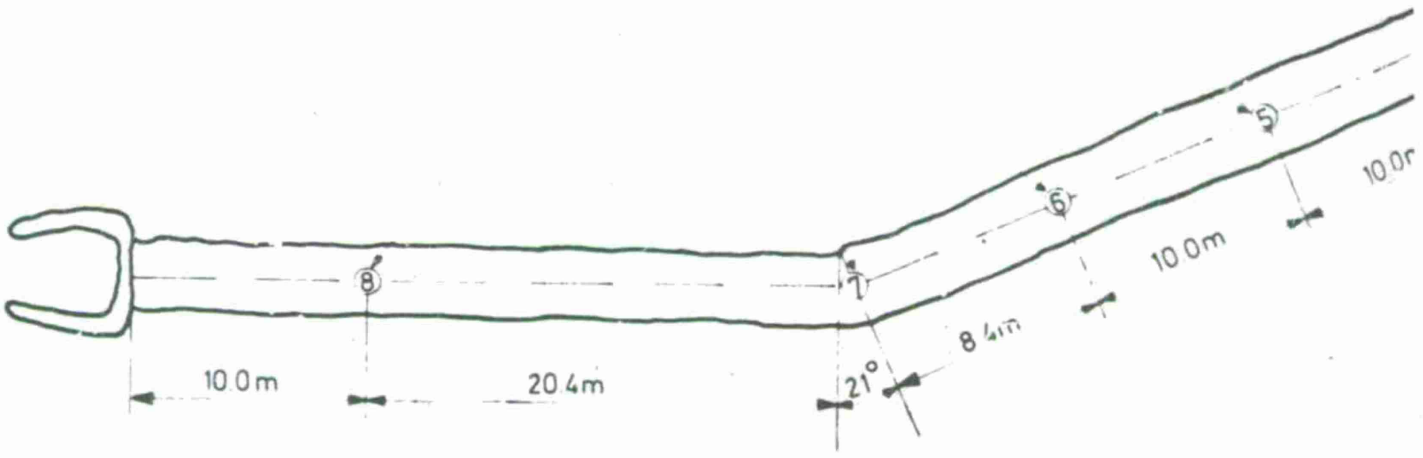

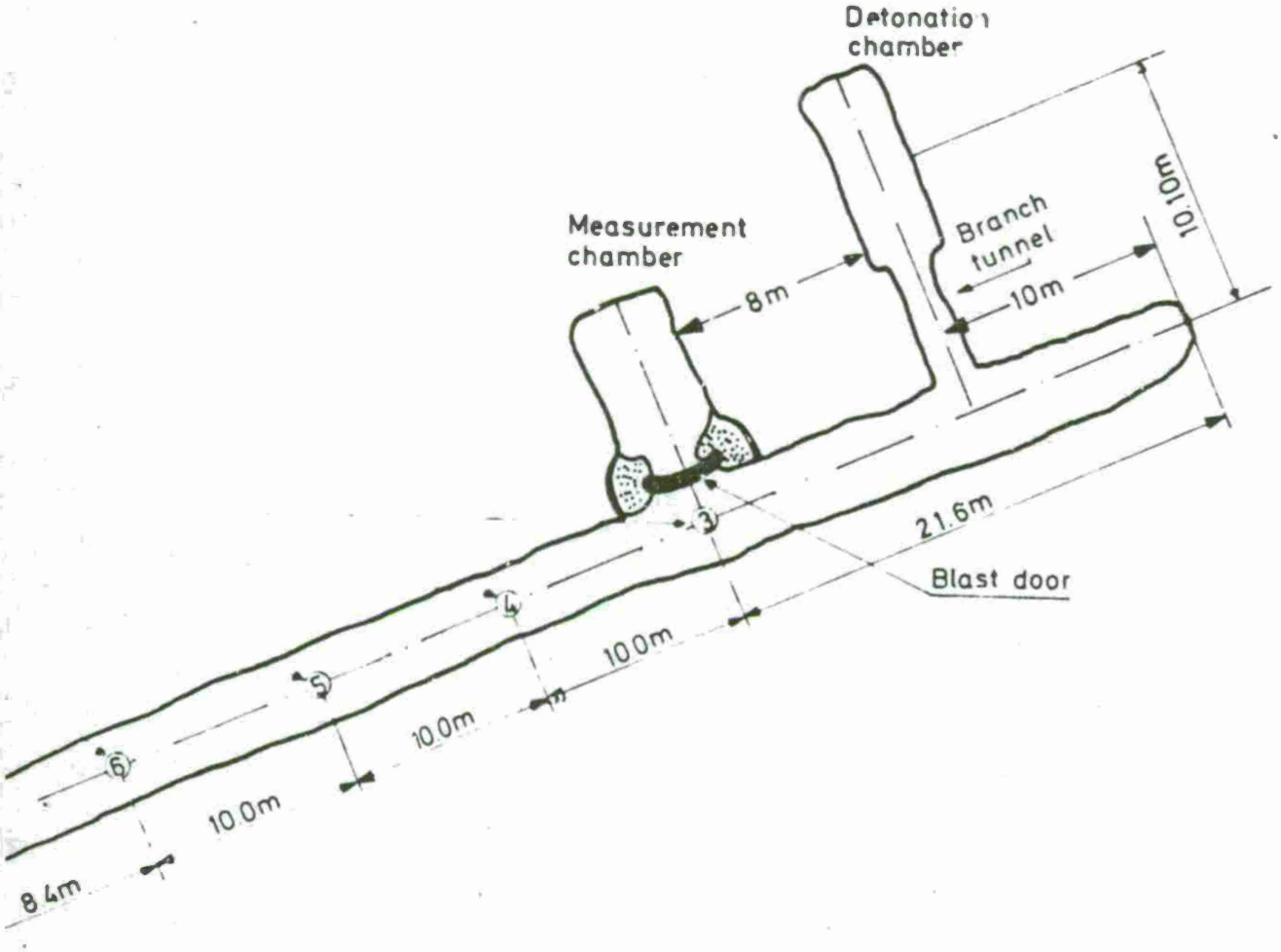
Detonation chamber
Measurement chamber
Branch tunnel
8m
10m
10.10m
21.6m
Blast door
10.0m
10.0m
10.0m
8.4m
1
2
3
4
5
6

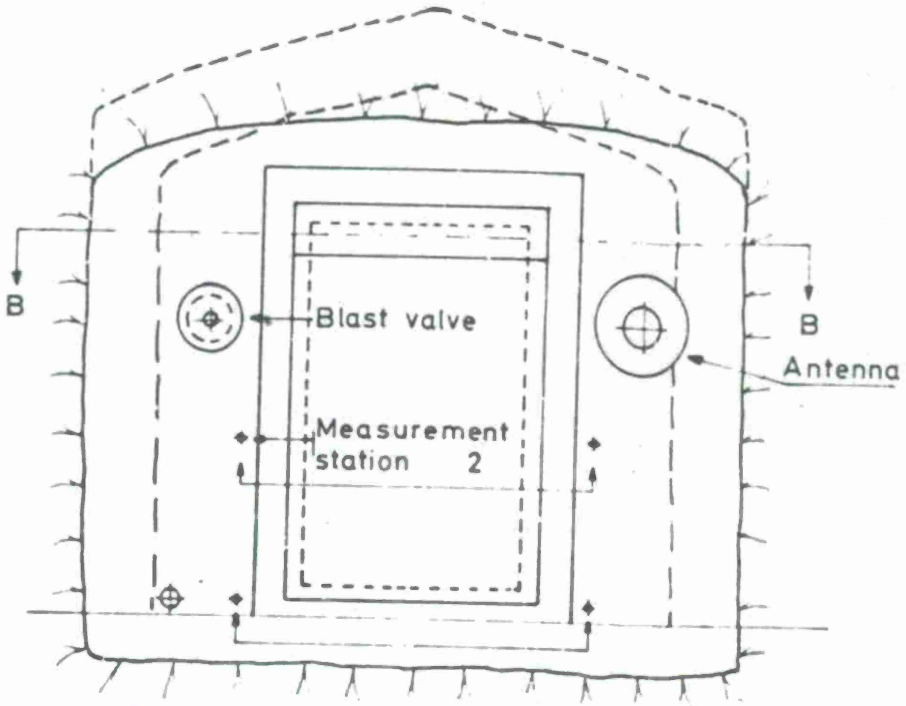

Section A-A, front view

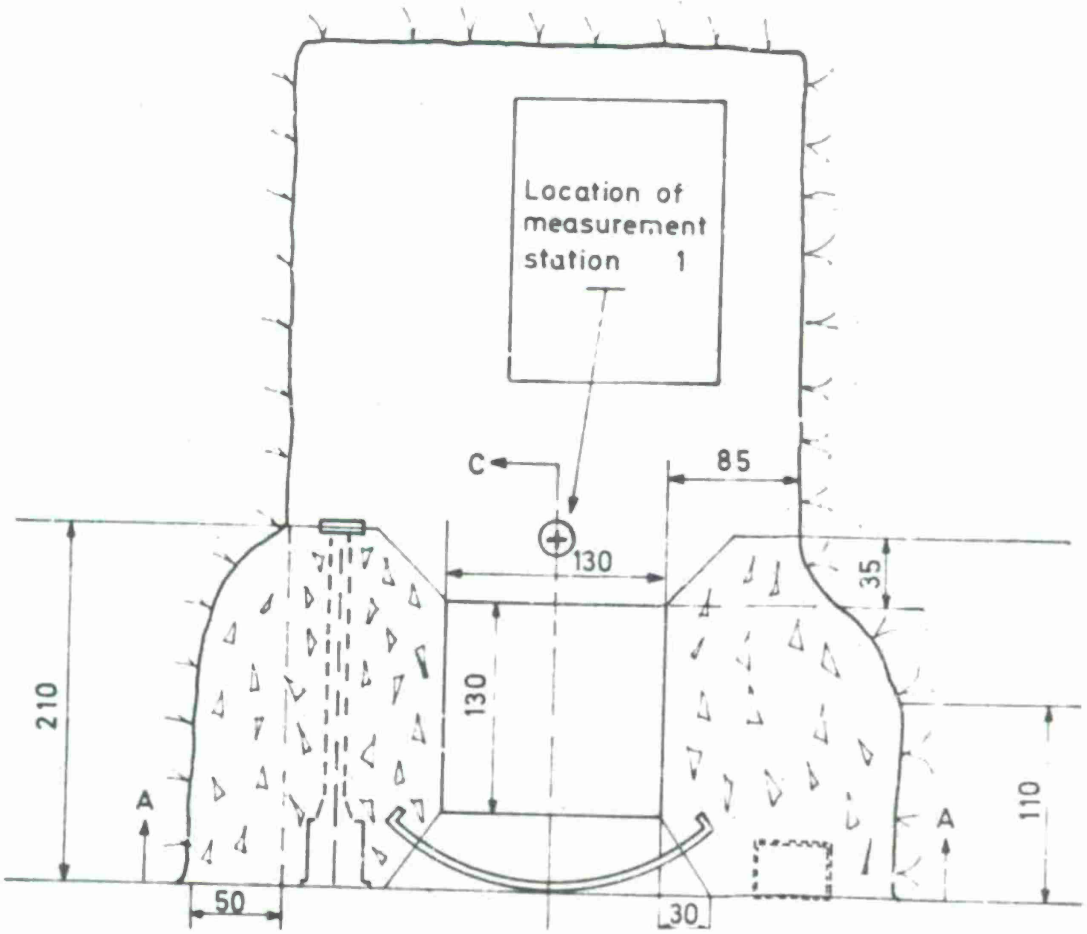

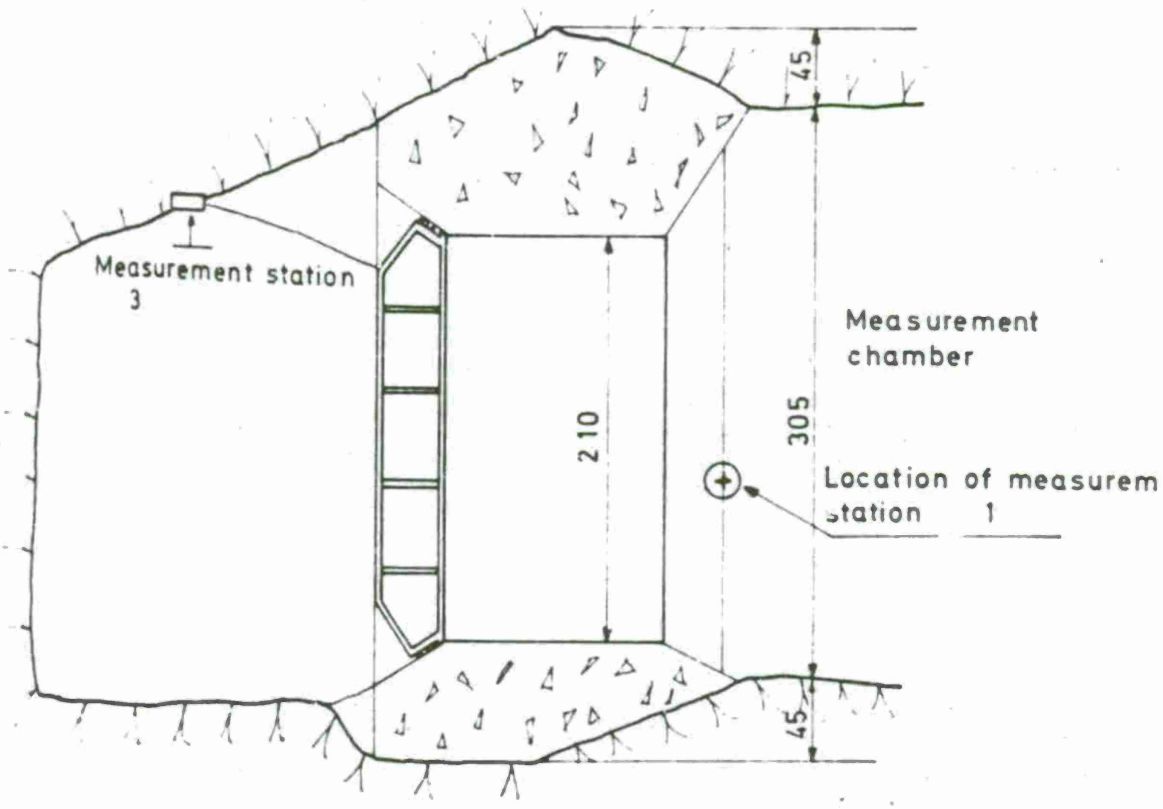

Section C-C, side view

Dimensions in cm

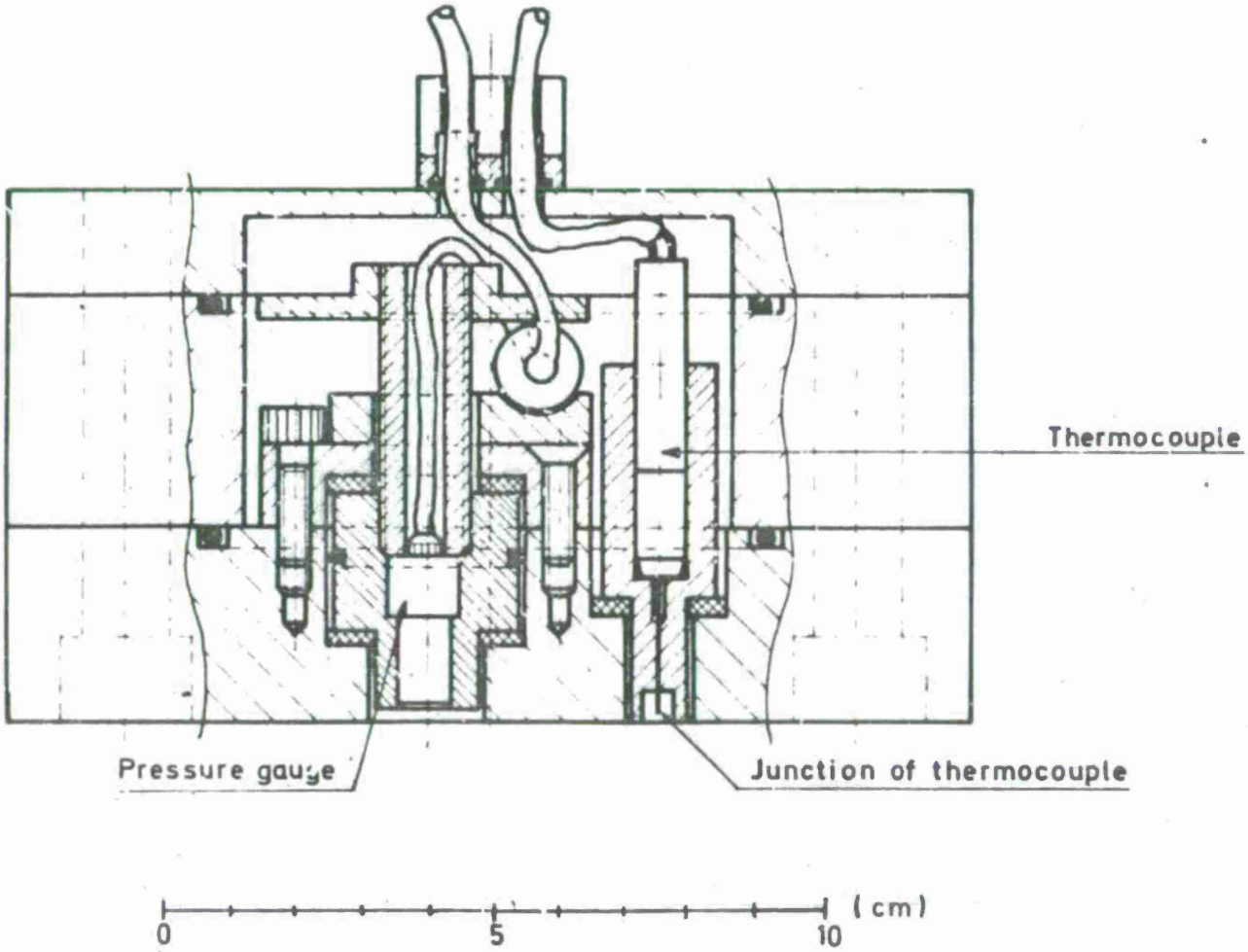

Figure 3.3 Measurement station situated in the roof

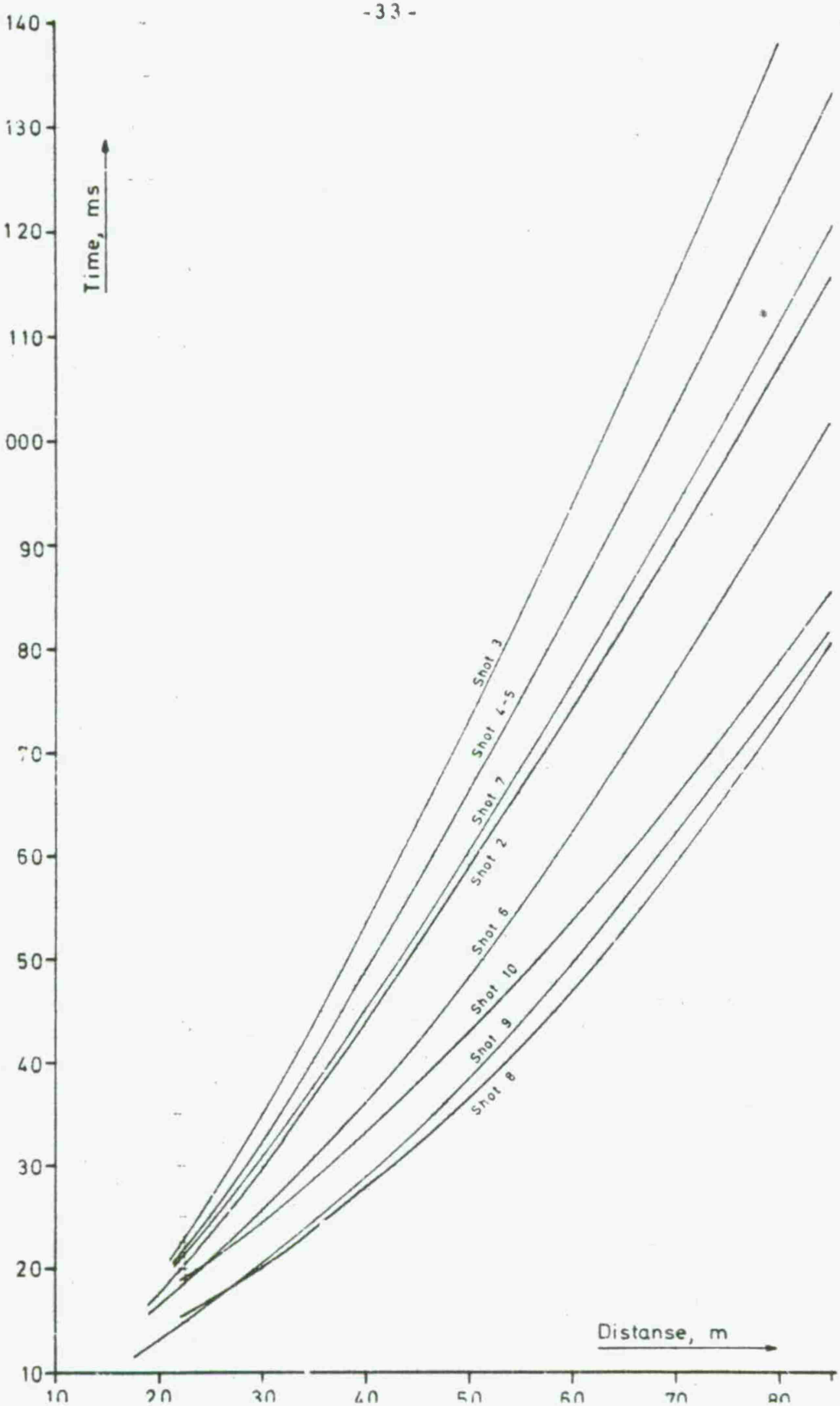
Time, ms
Distanse, m
Shot 3
Shot 4-5
Shot 7
Shot 2
Shot 6
Shot 10
Shot 9
Shot 8
140
130
120
110
000
90
80
70
60
50
40
30
20
10
10
20
30
40
50
60
70
80

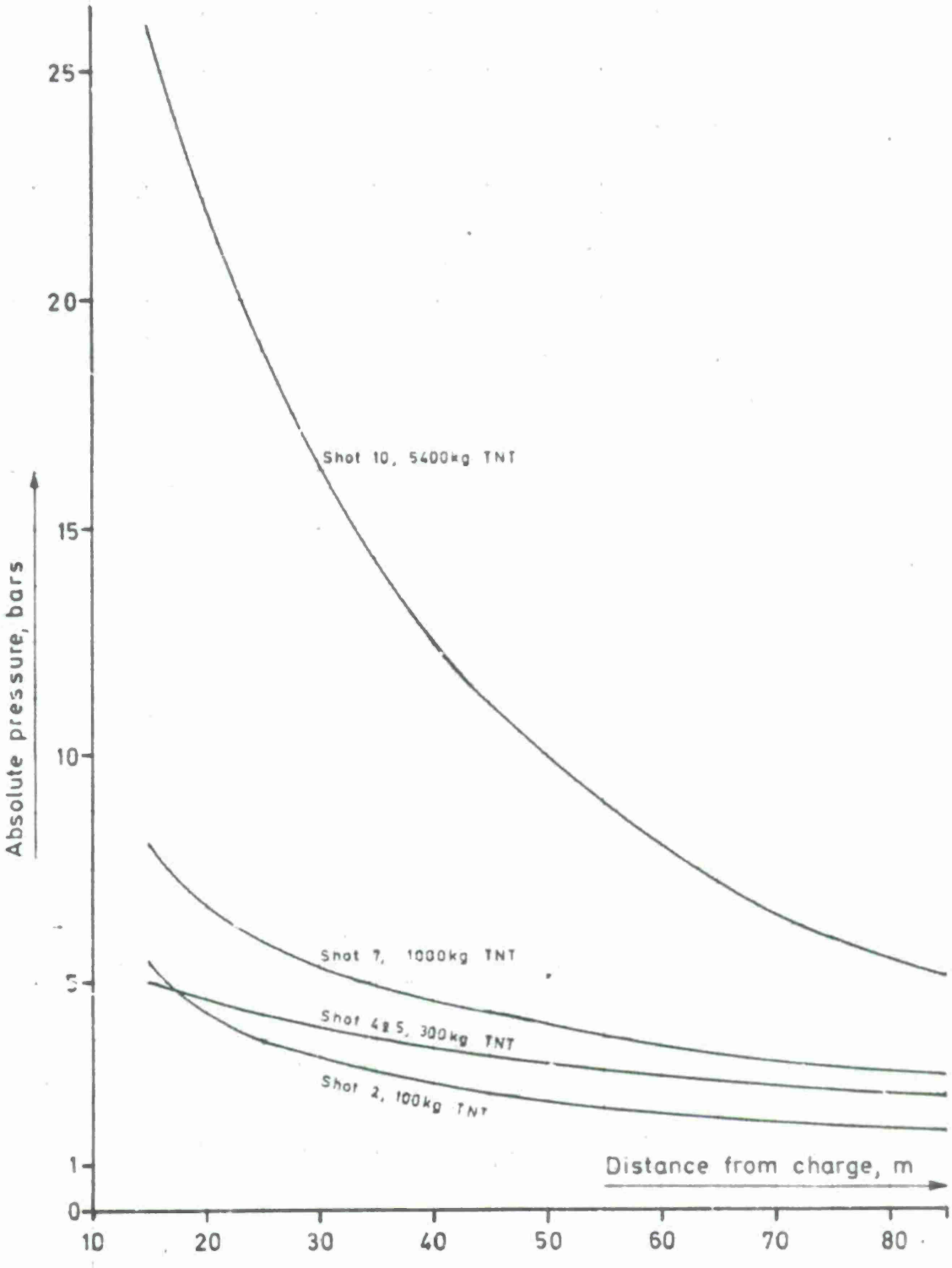

Fig. 3.5 Blast pressure derivel from the arrival times for charges fired in the chamber

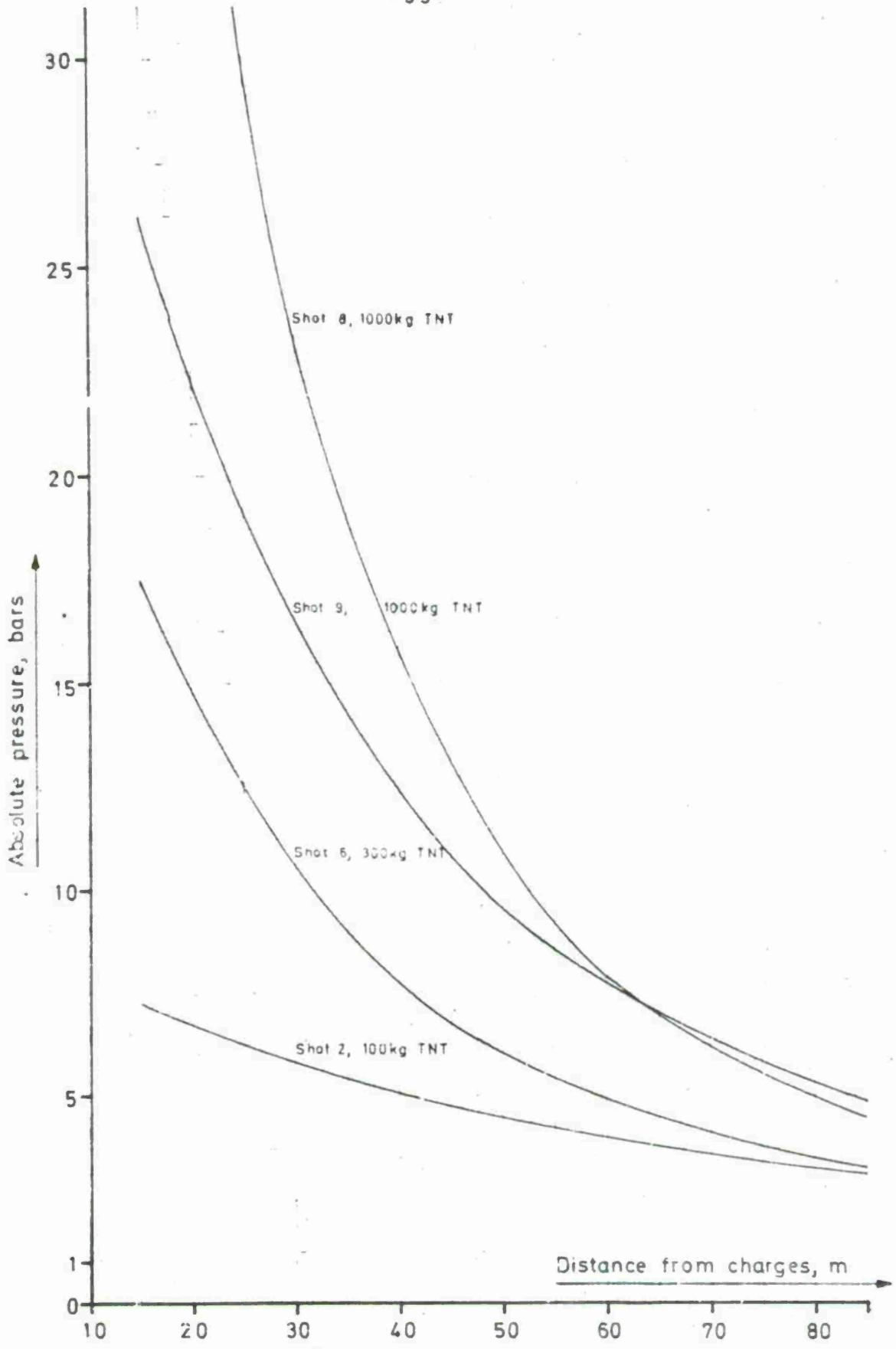
Absolute pressure, bars
30
25
20
15
10
5
1
0
Shot 8, 1000kg TNT
Shot 9, 1000kg TNT
Shot 6, 300kg TNT
Shot 2, 100kg TNT
Distance from charges, m
10
20
30
40
50
60
70
80

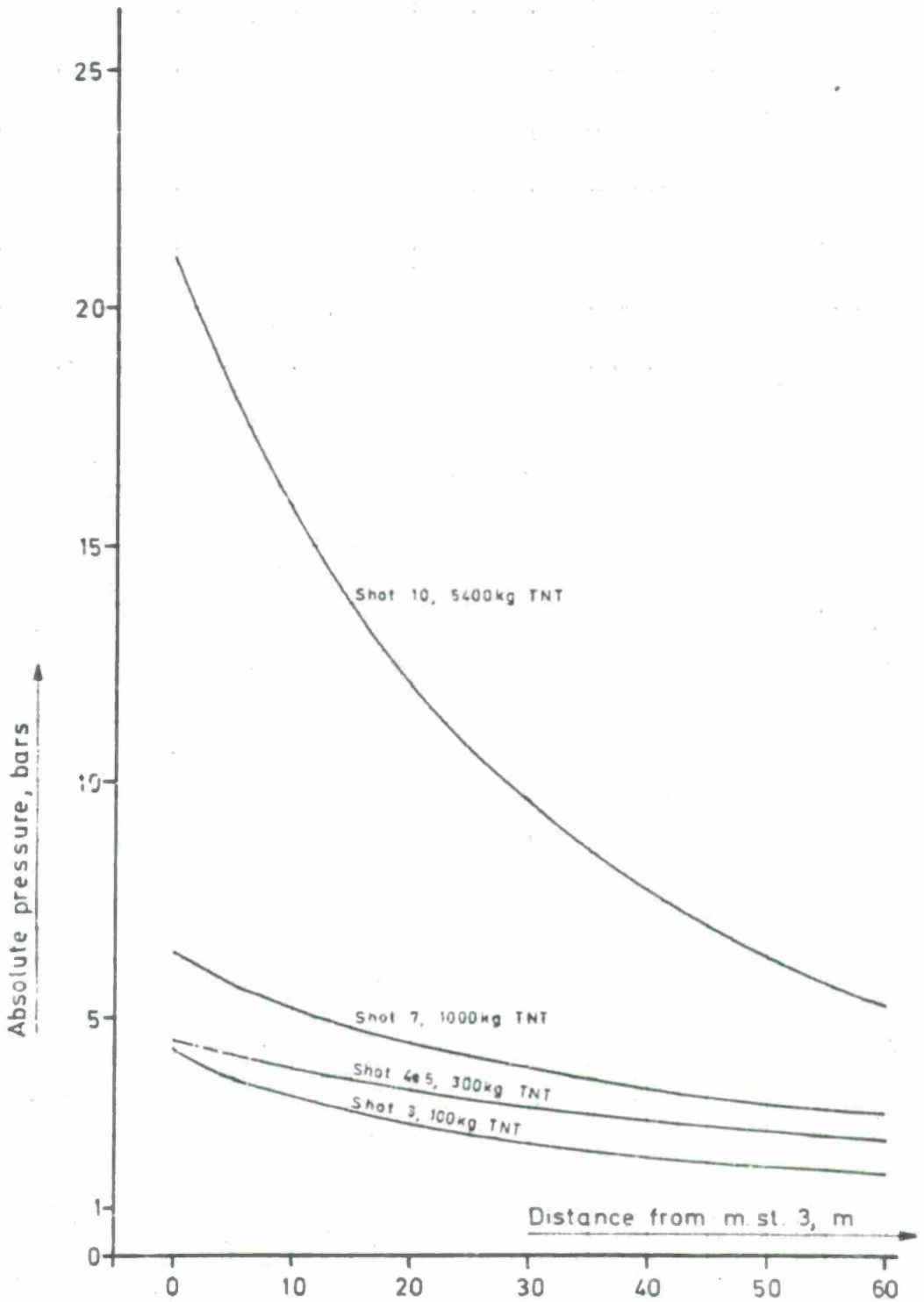

Fig. 3.7 Blast pressure derived from the arrival times for charges fired in the chamber

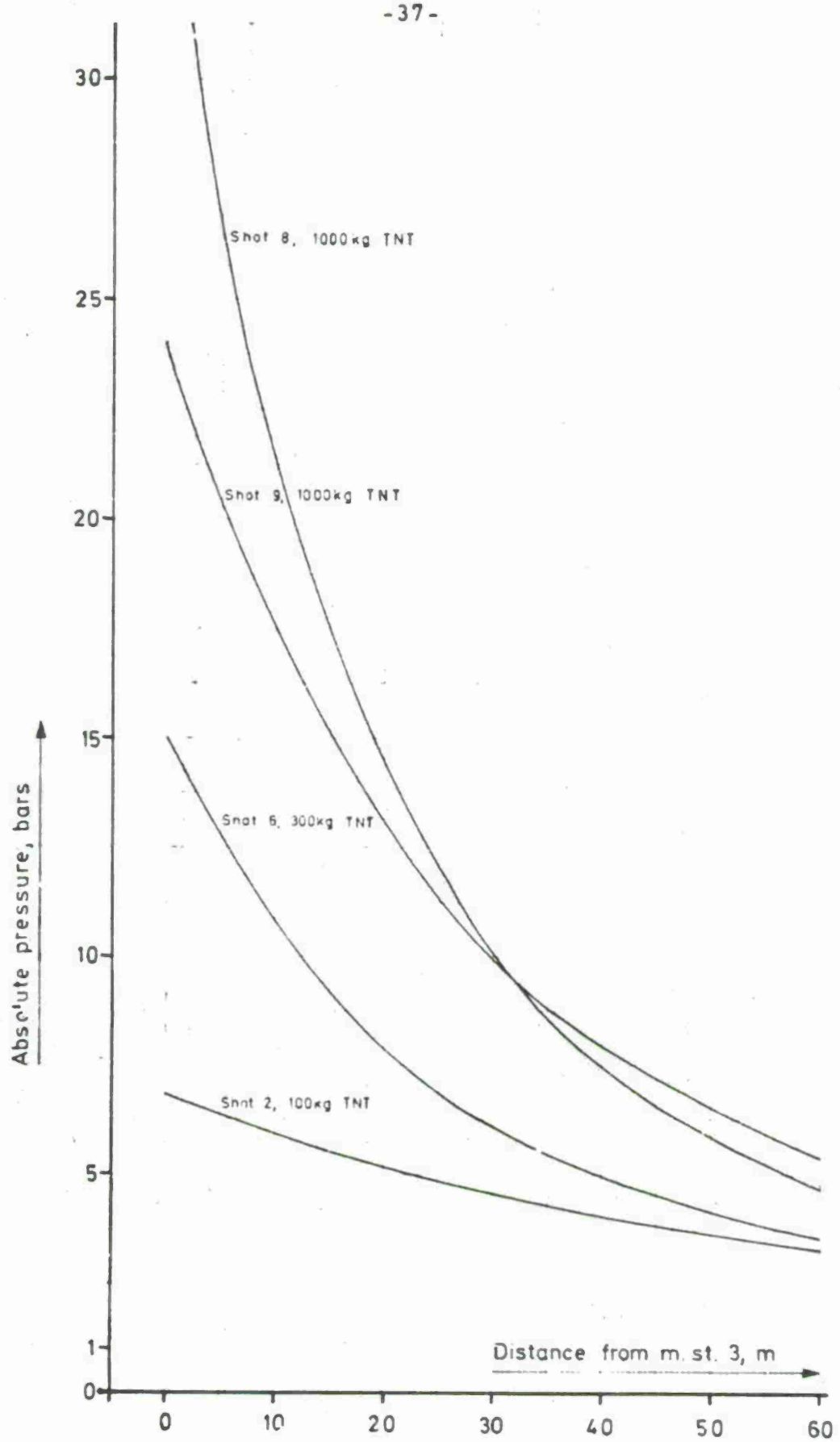
Shot 8, 1000kg TNT
Shot 9, 1000kg TNT
Shot 6, 300kg TNT
Shot 2, 100kg TNT
Absolute pressure, bars
Distance from m. st. 3, m
30
25
20
15
10
5
1
0
0
10
20
30
40
50
60

Shot 2 - 100kg TNT - Tunnel

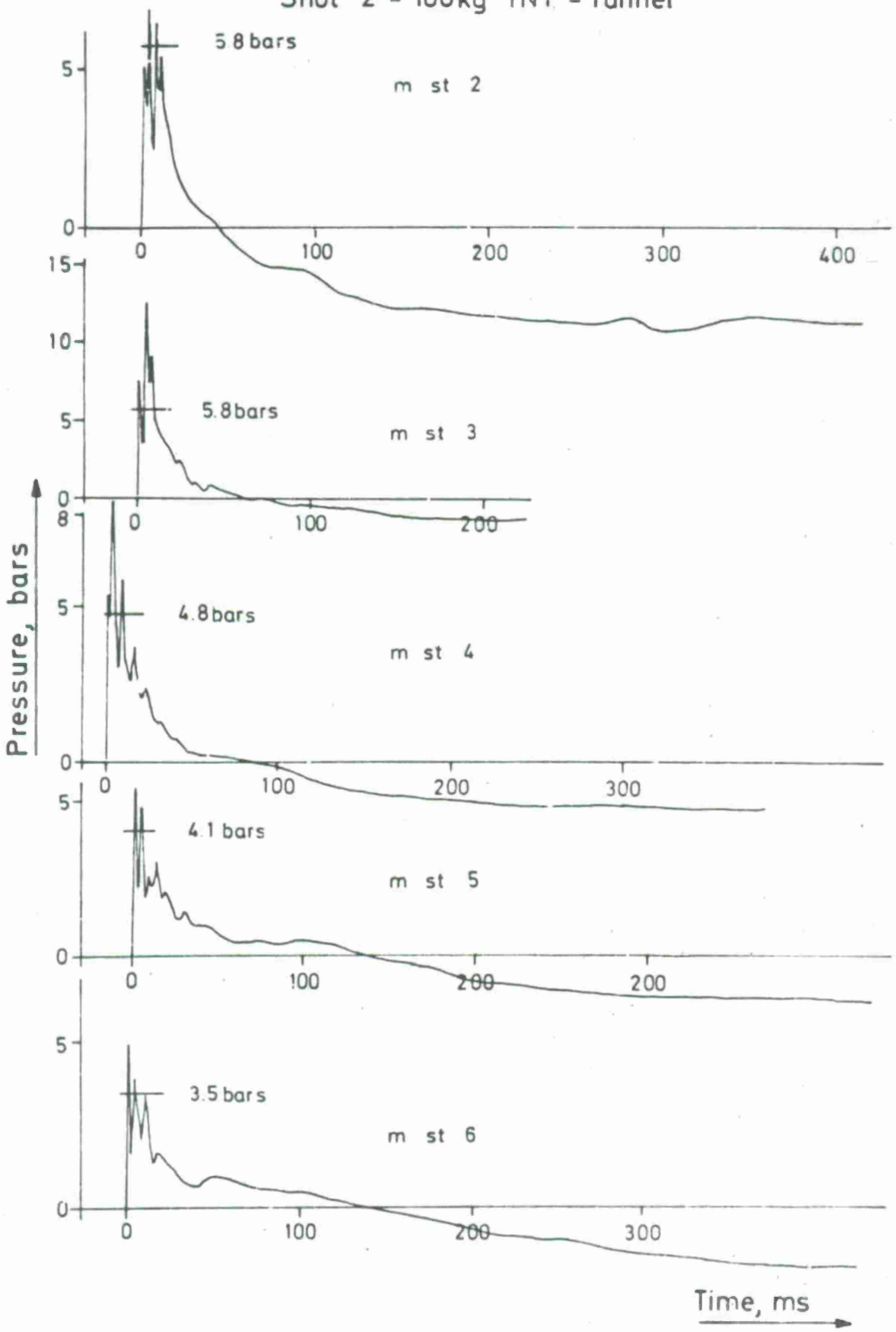

Shot 3 - 100kg TNT - Chamber

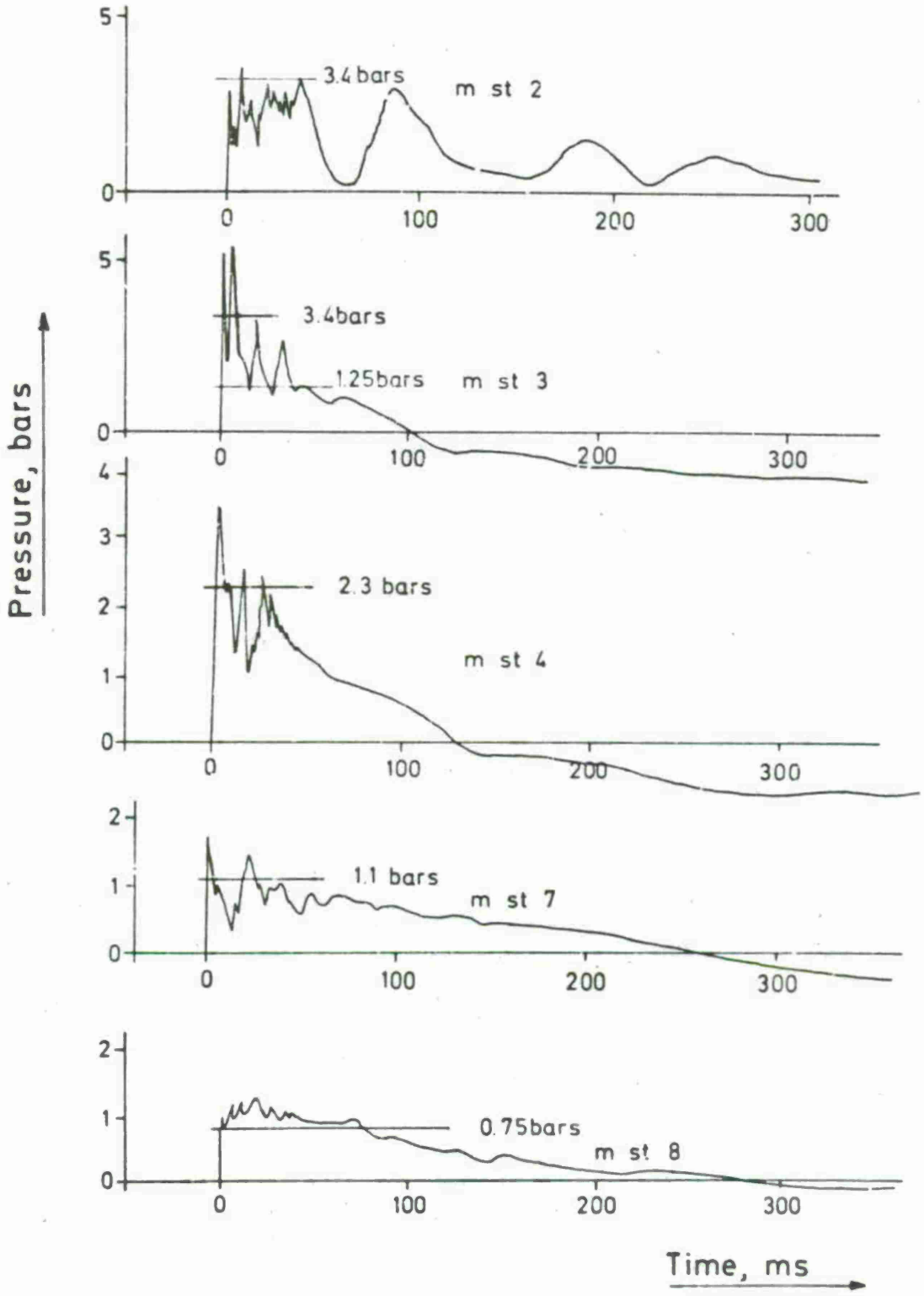

Fig. 3.10 Measured overpressure

Shot 4 - 300kg TNT - Chamber

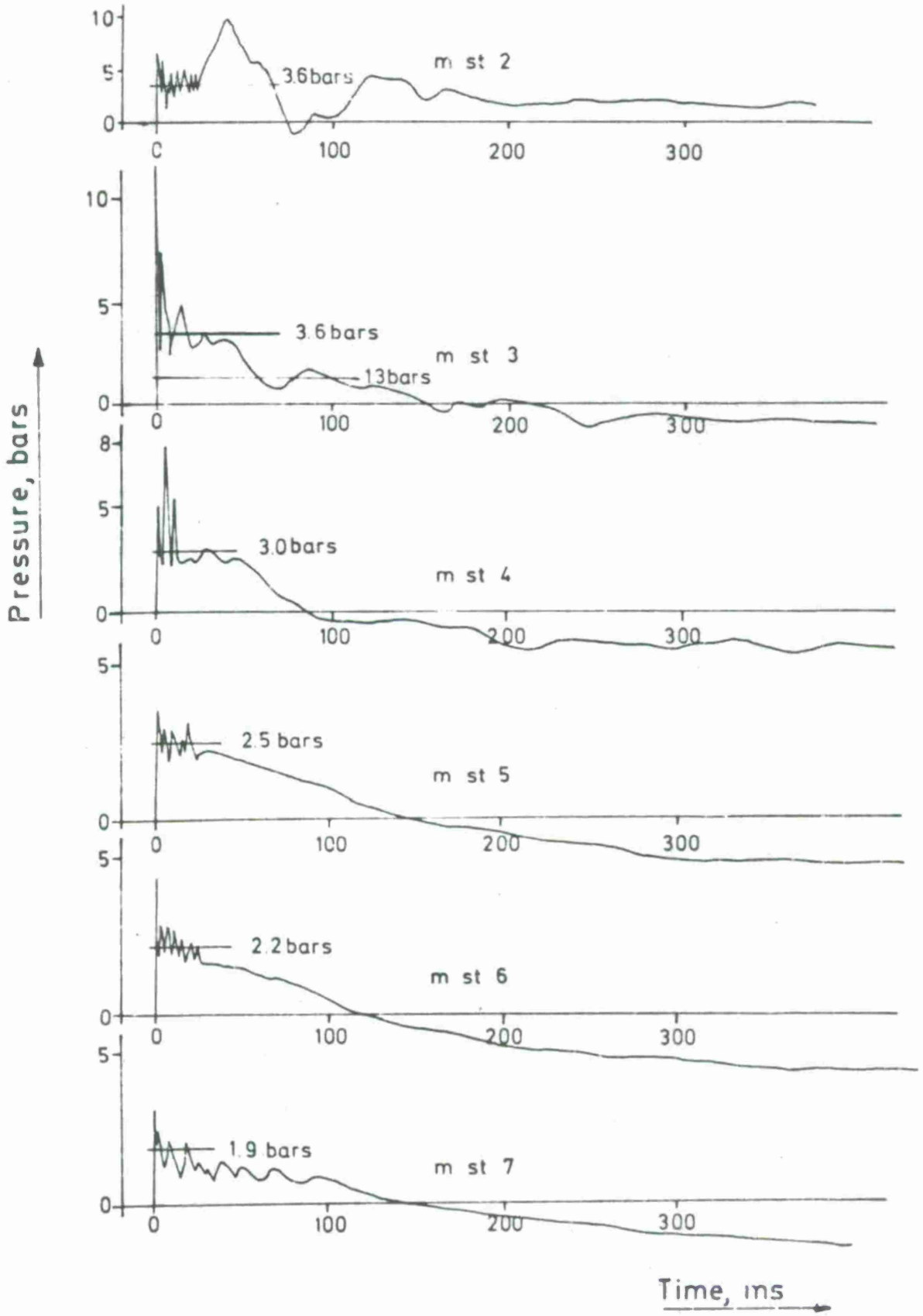

Shot 5 - 300kg TNT - Chamber

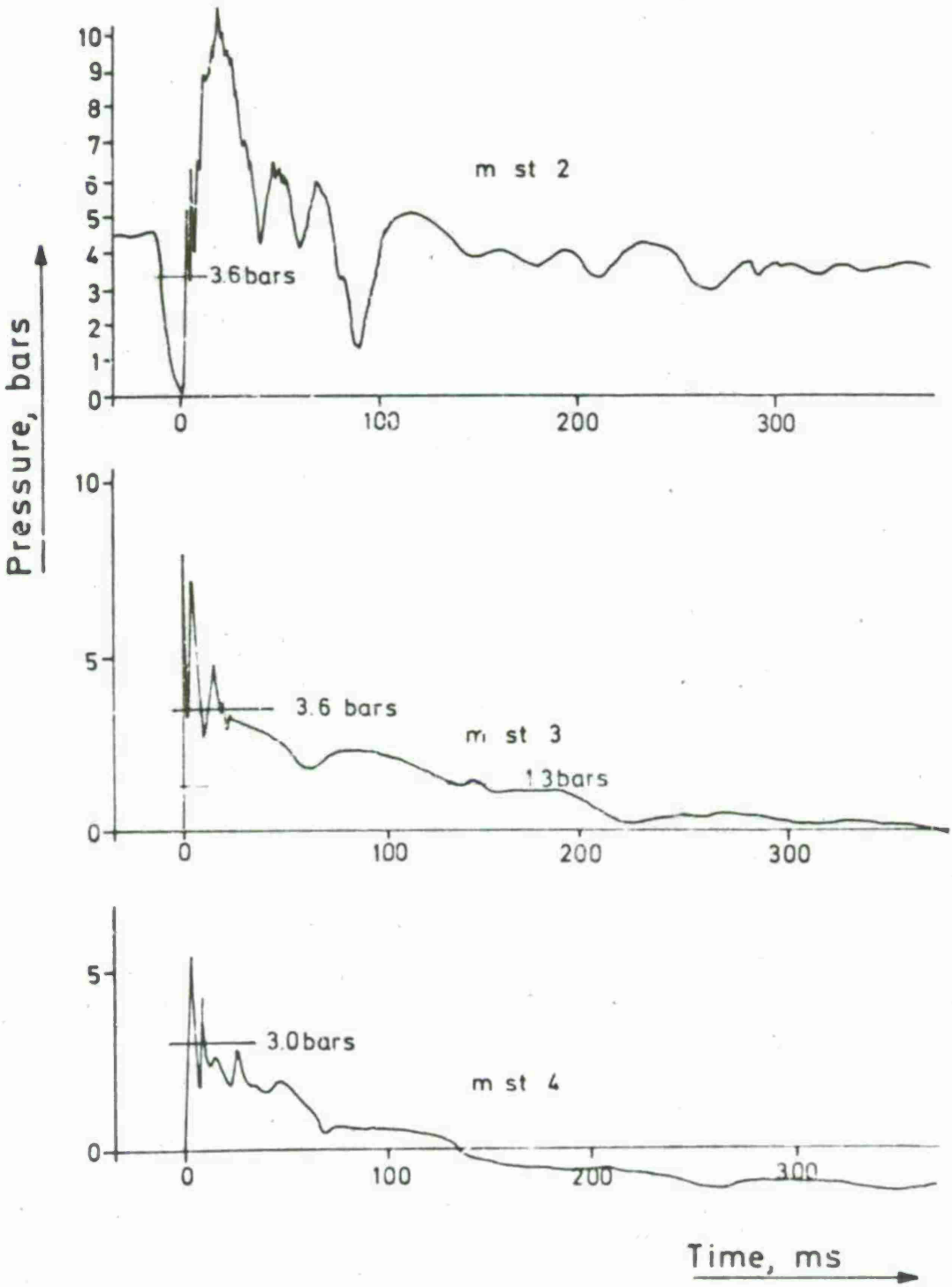

Fig. 3.12 Measured overpressure

Shot 5 - 300kg TNT - Chamber

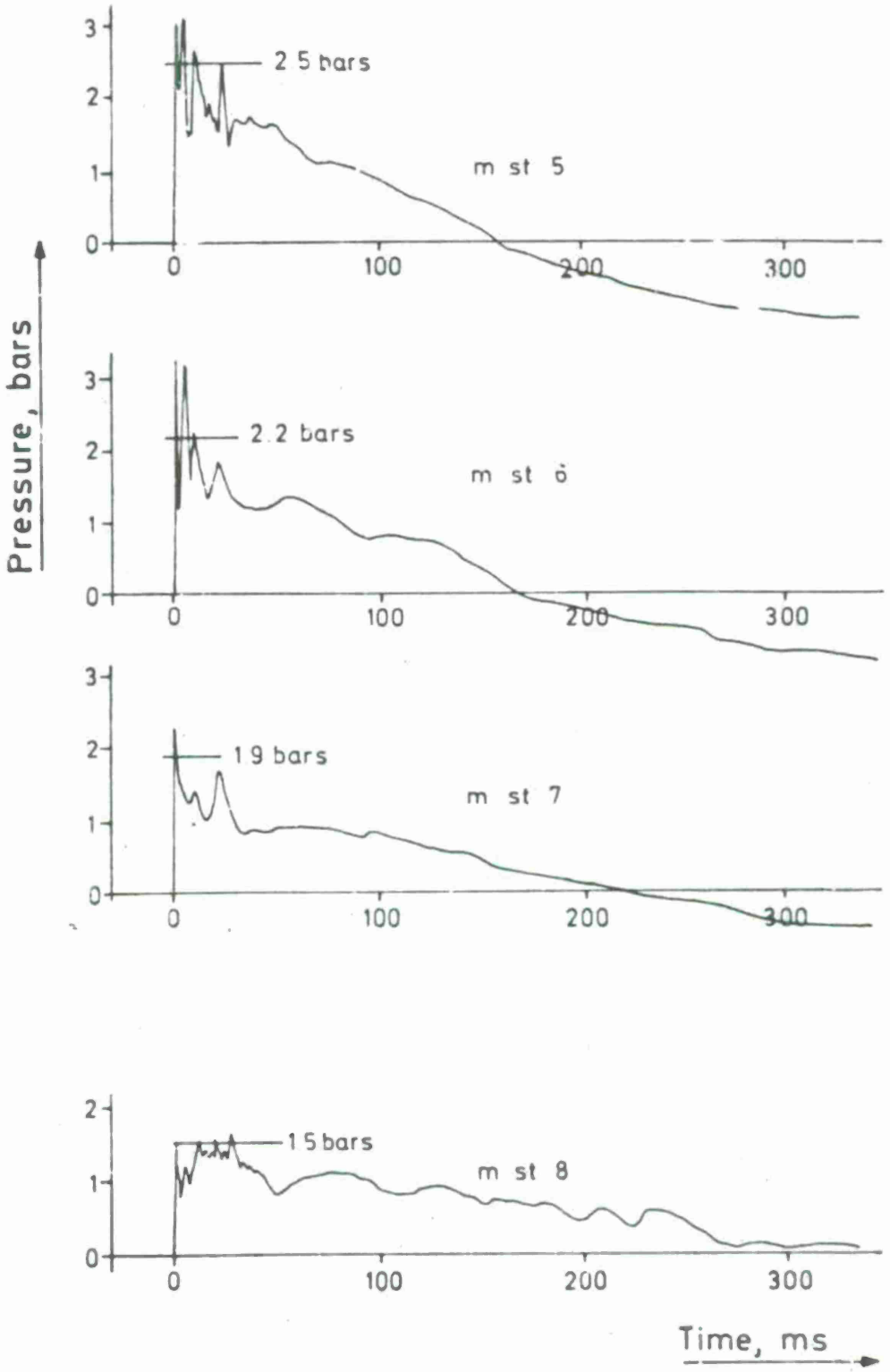

Fig. 3.13 Measured overpressure

Shot 6 – 300kg TNT - Tunnel

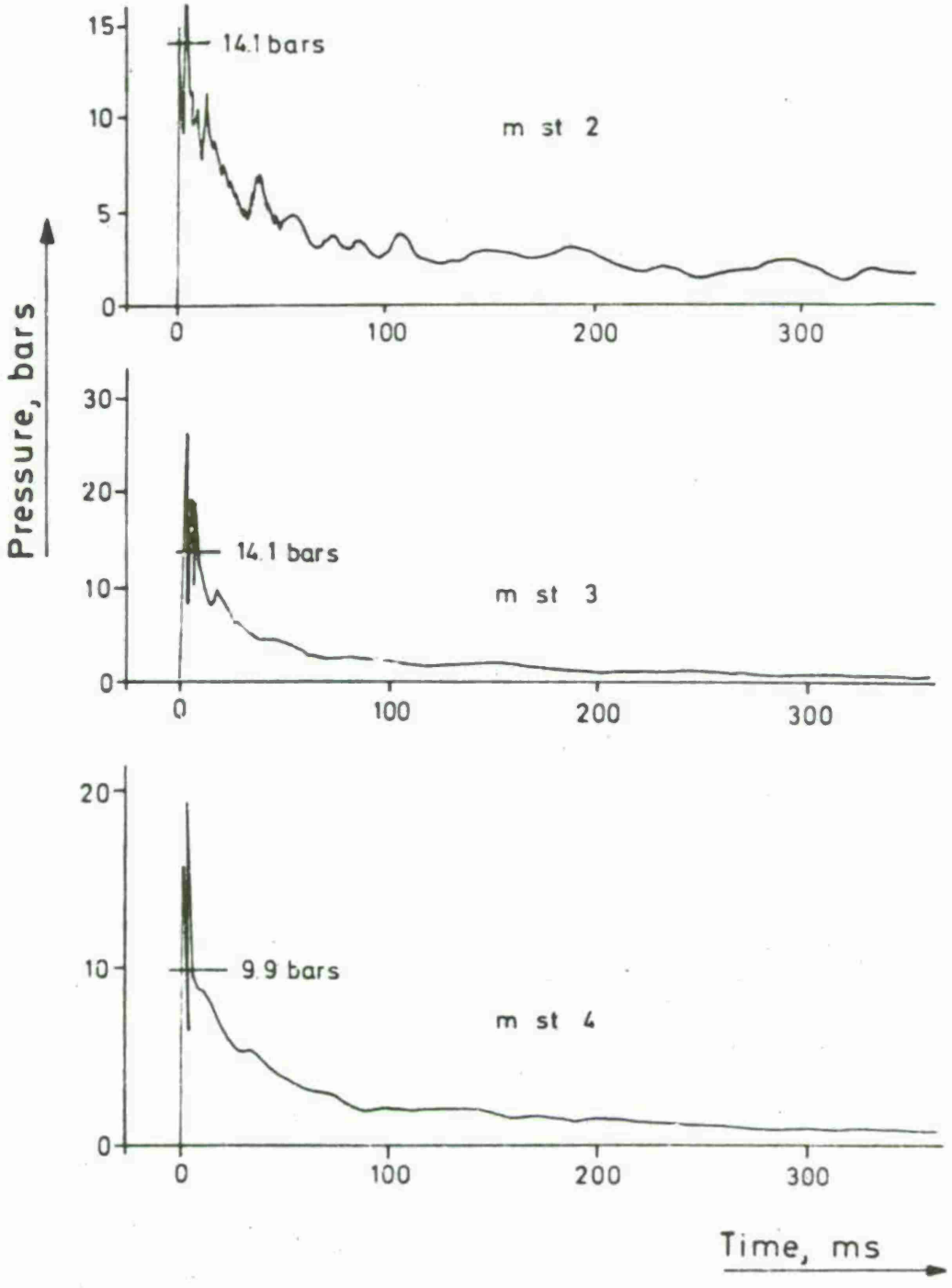

Shot 6 - 300kg TNT - Tunnel

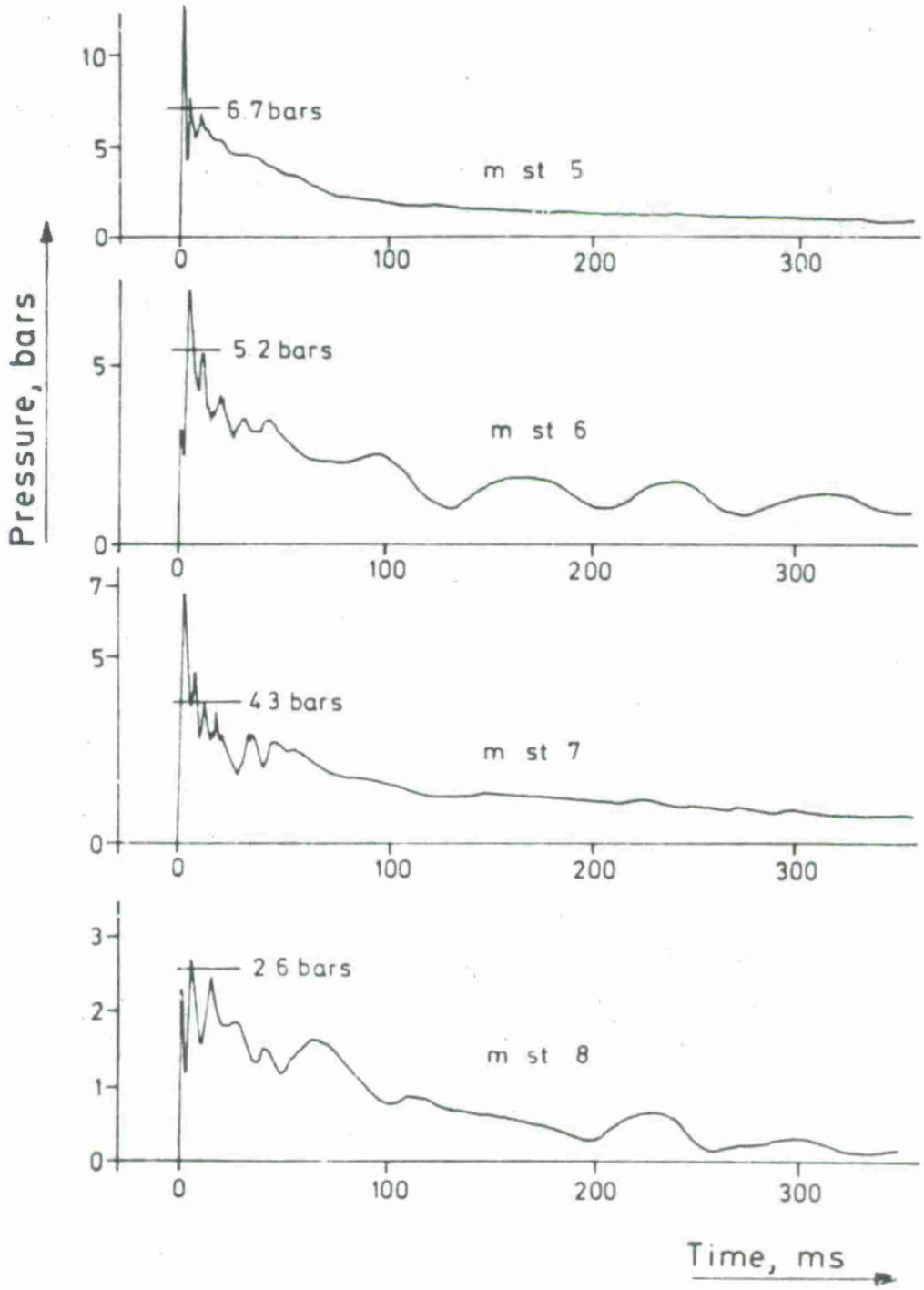

Fig. 3.15 Measured overpressure

Shot 7 - 1000kg TNT - Chamber

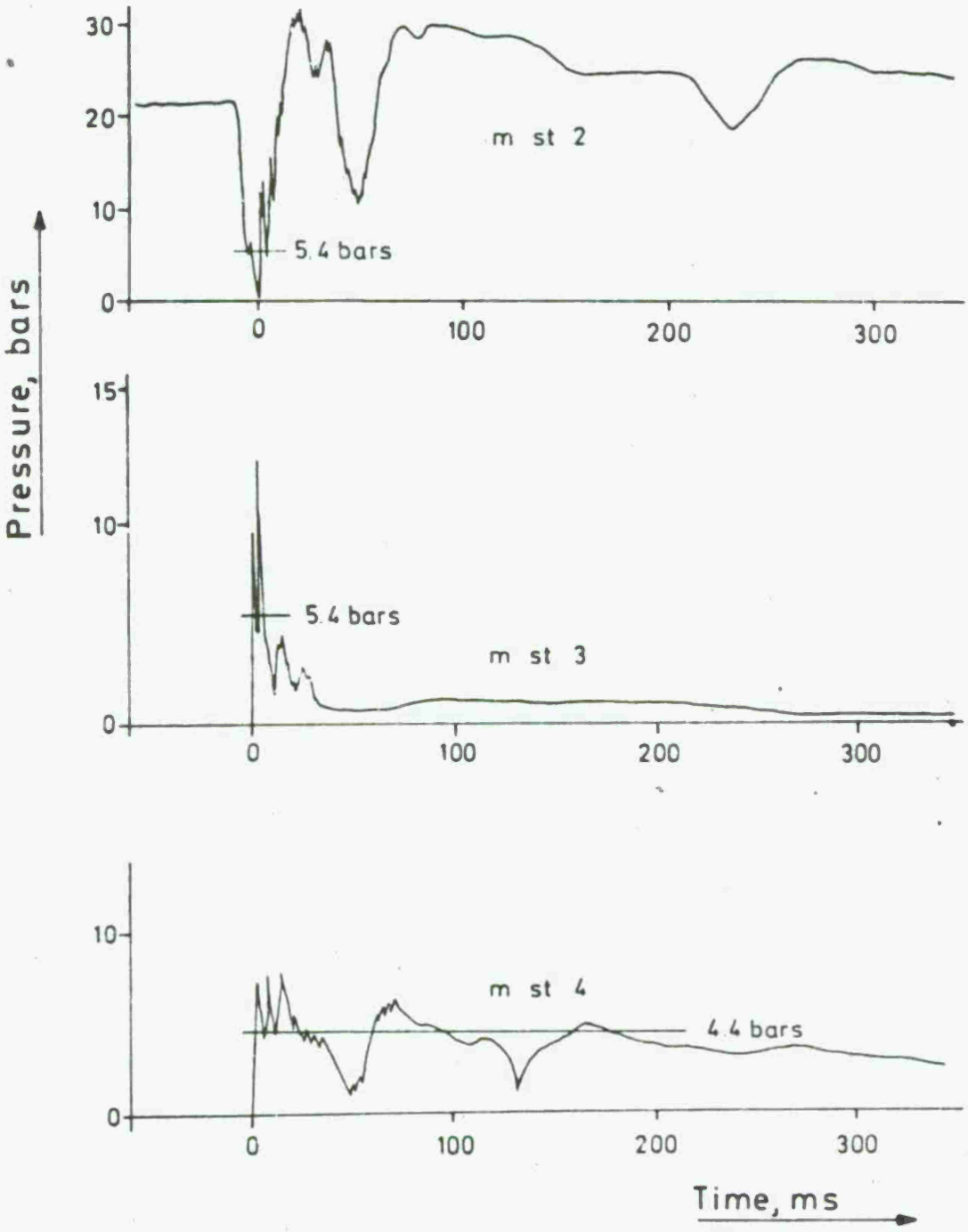

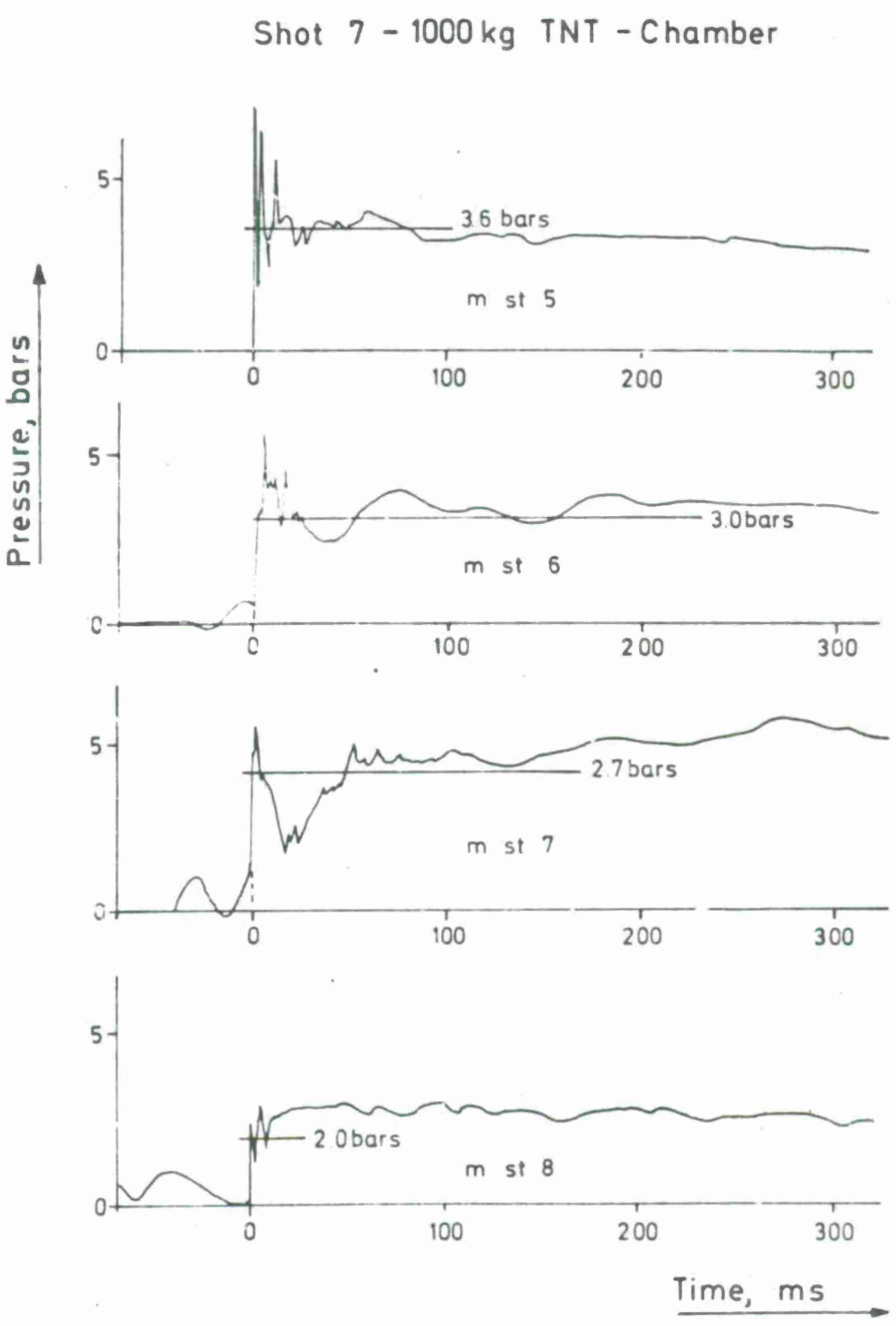

Fig. 3.17 Measured overpressure

Shot 8 - 1000kg TNT - Tunnel

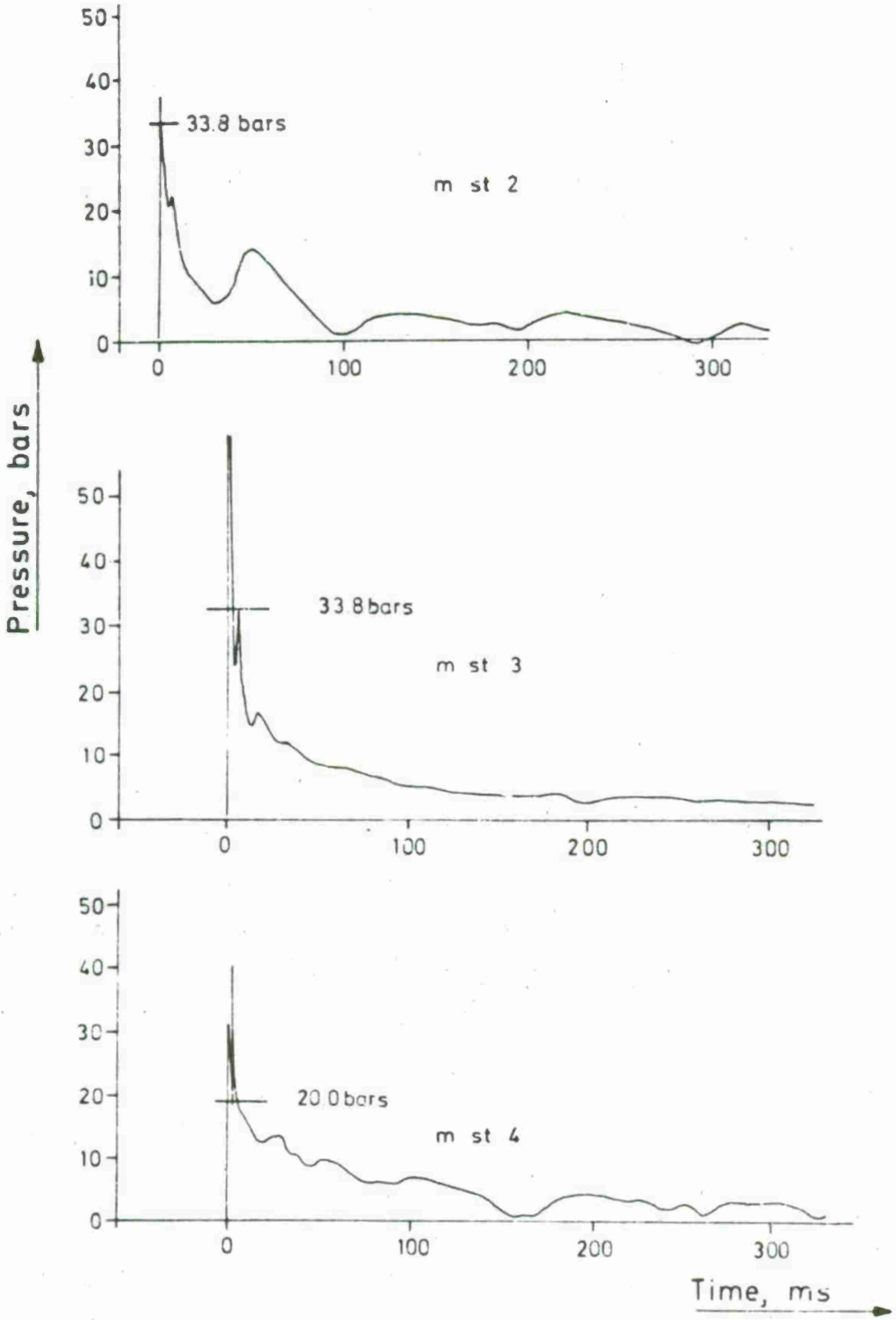

Shot 8 - 1000kg TNT - Tunnel

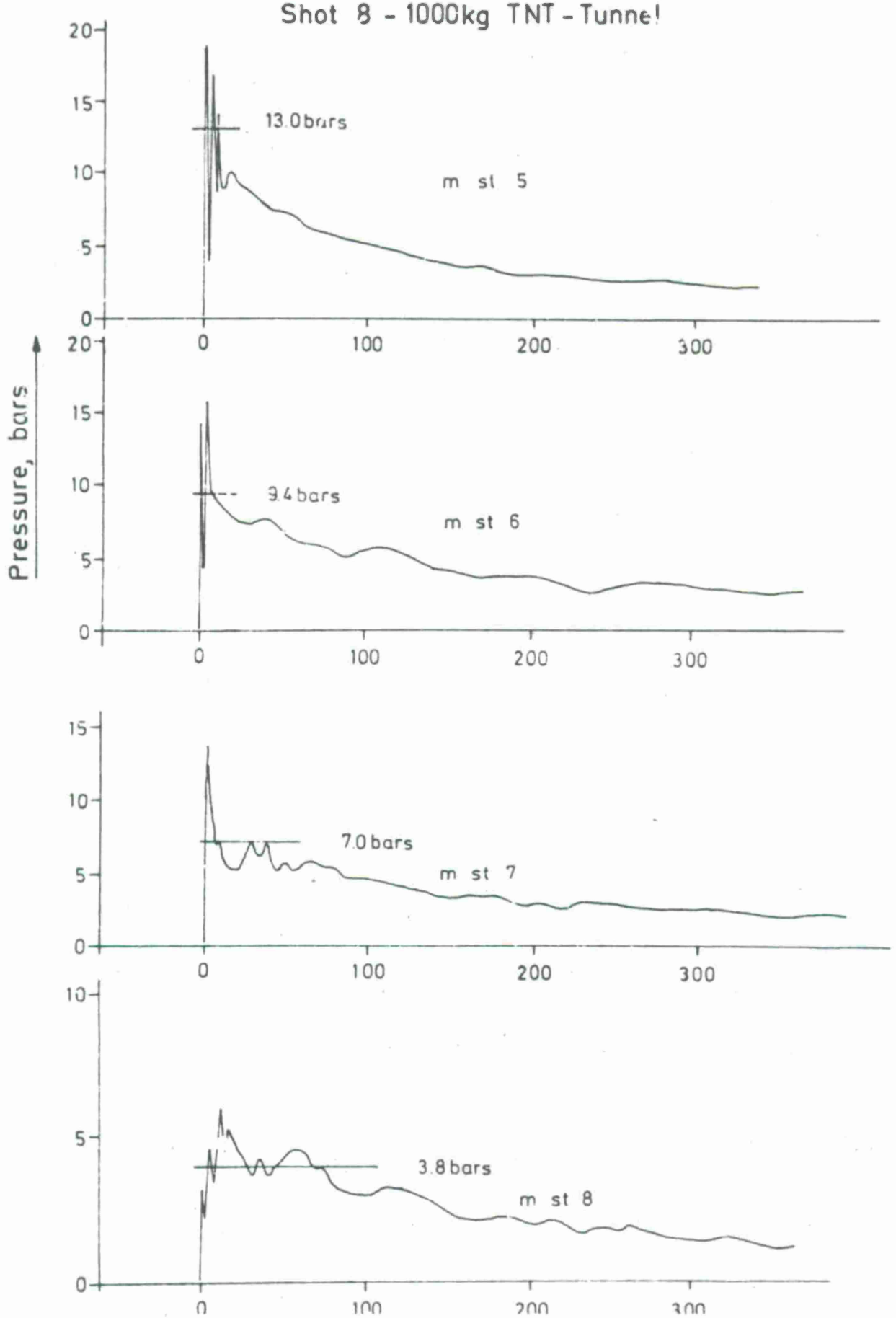

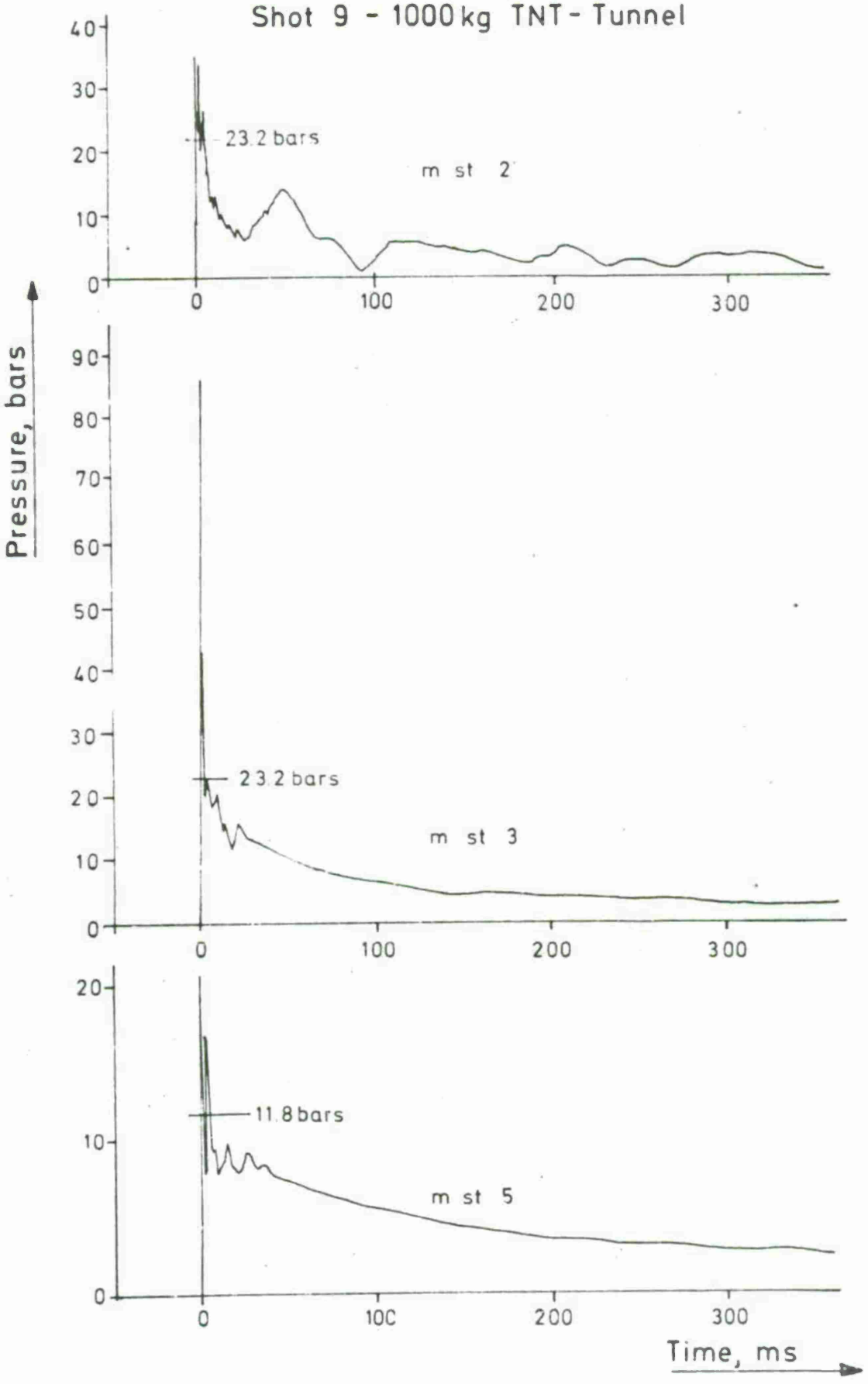
Shot 9 - 1000 kg TNT - Tunnel
Pressure, bars
23.2 bars
m st 2
23.2 bars
m st 3
11.8 bars
m st 5
Time, ms

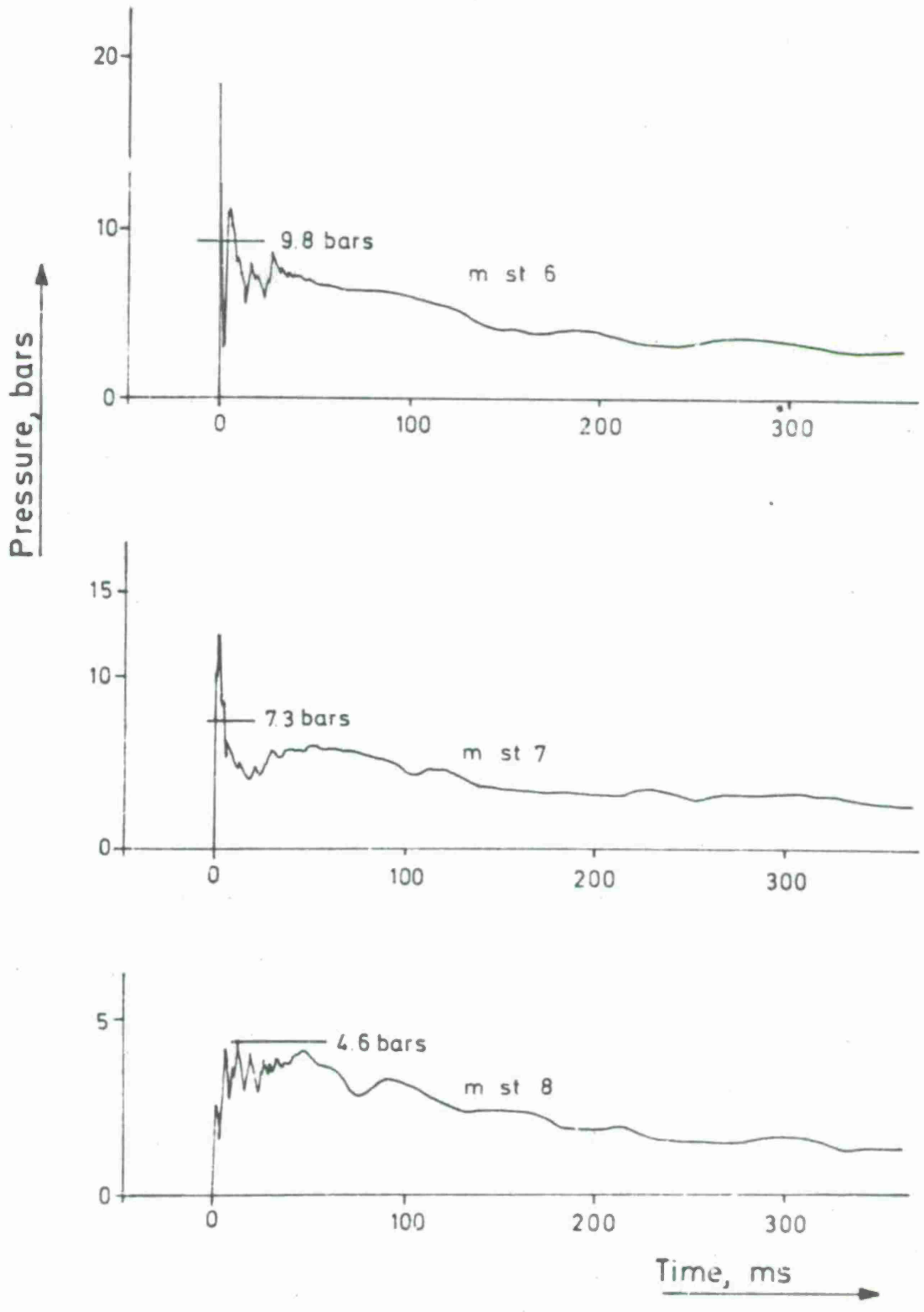

Fig. 3.21 Measured overpressure

Shot 10 - 5400 kg TNT - Chamber

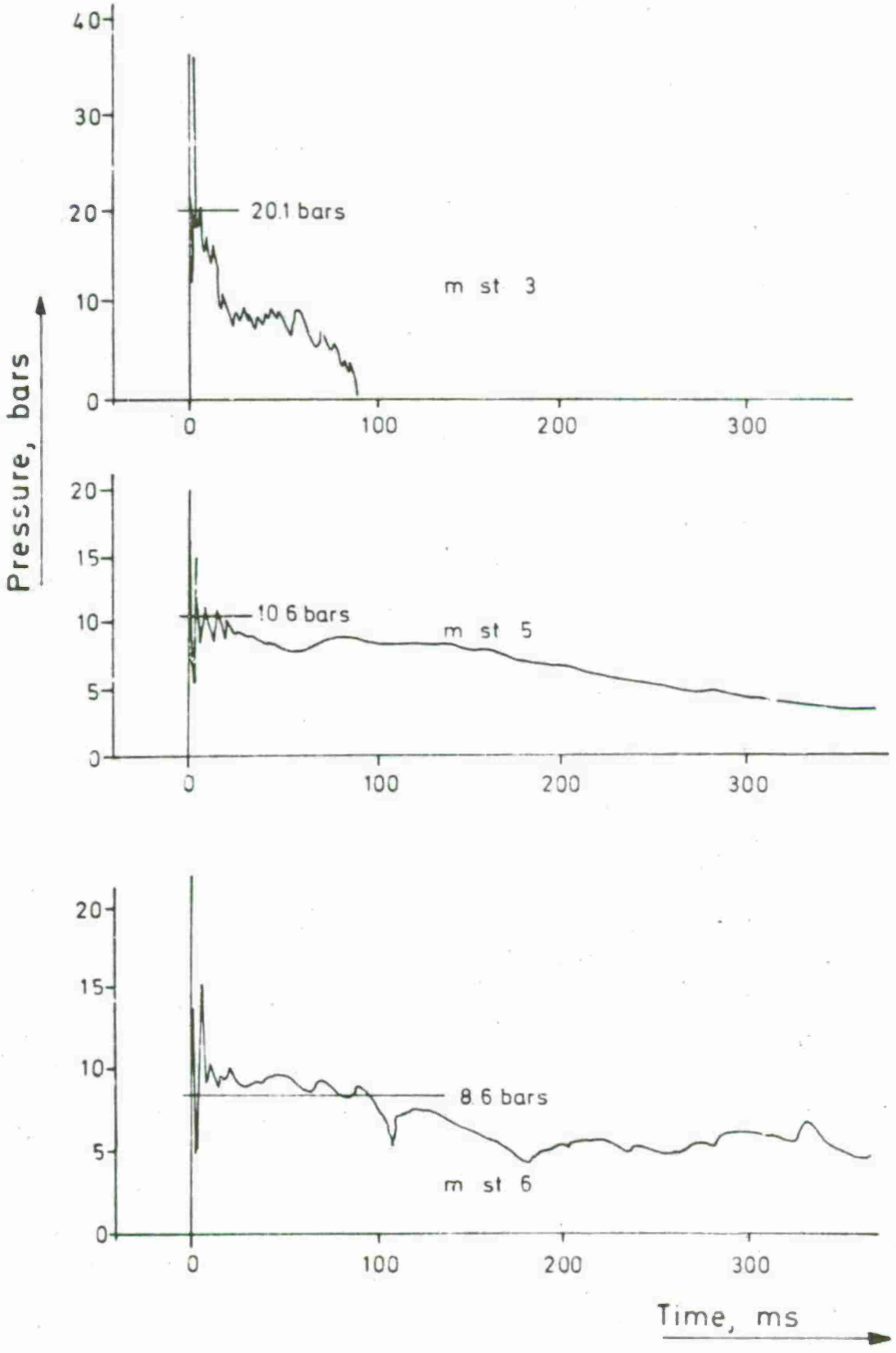

Shot 10 - 5400 kg TNT - Chamber

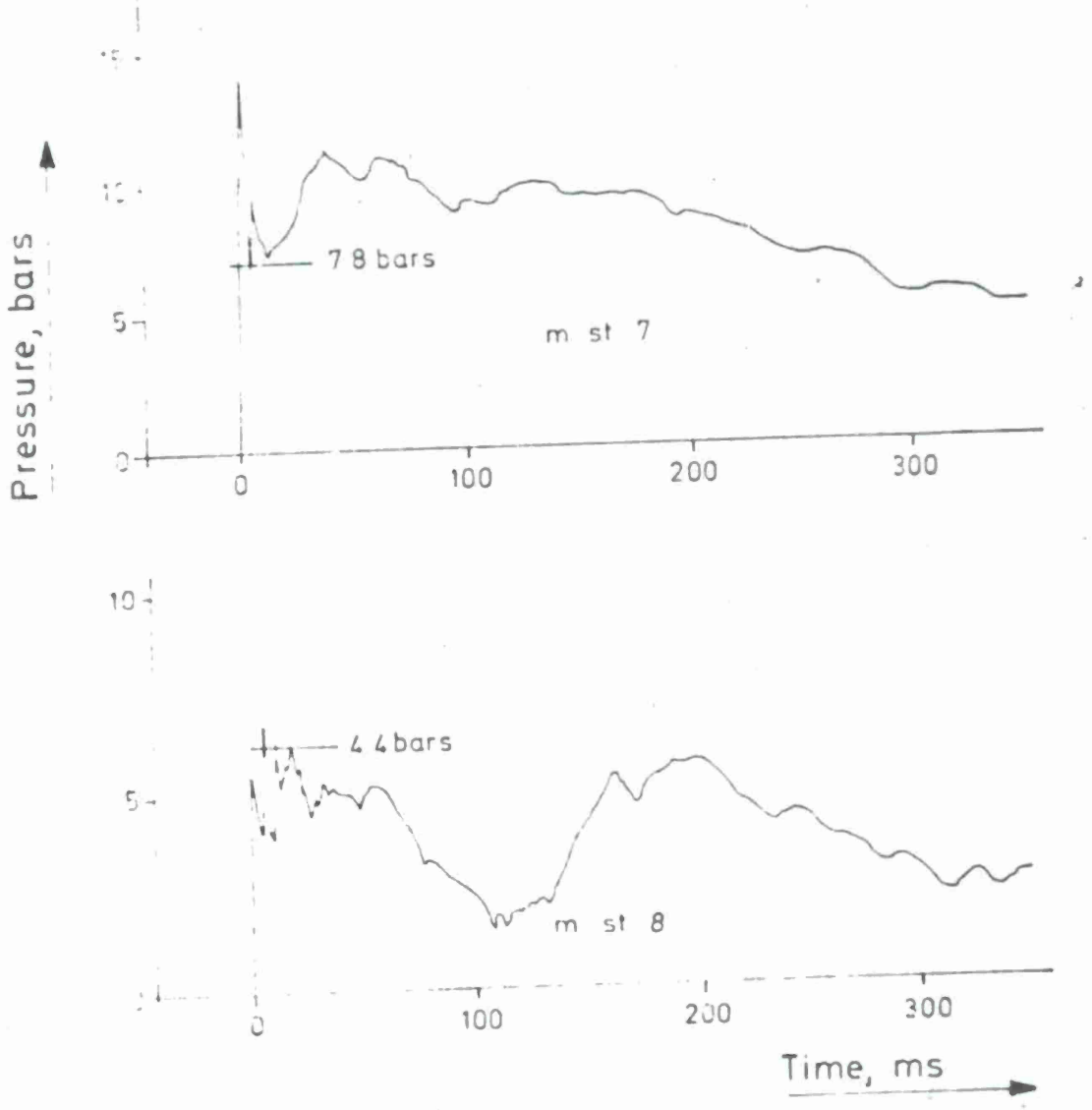

Fig 3.23 Measured overpressure

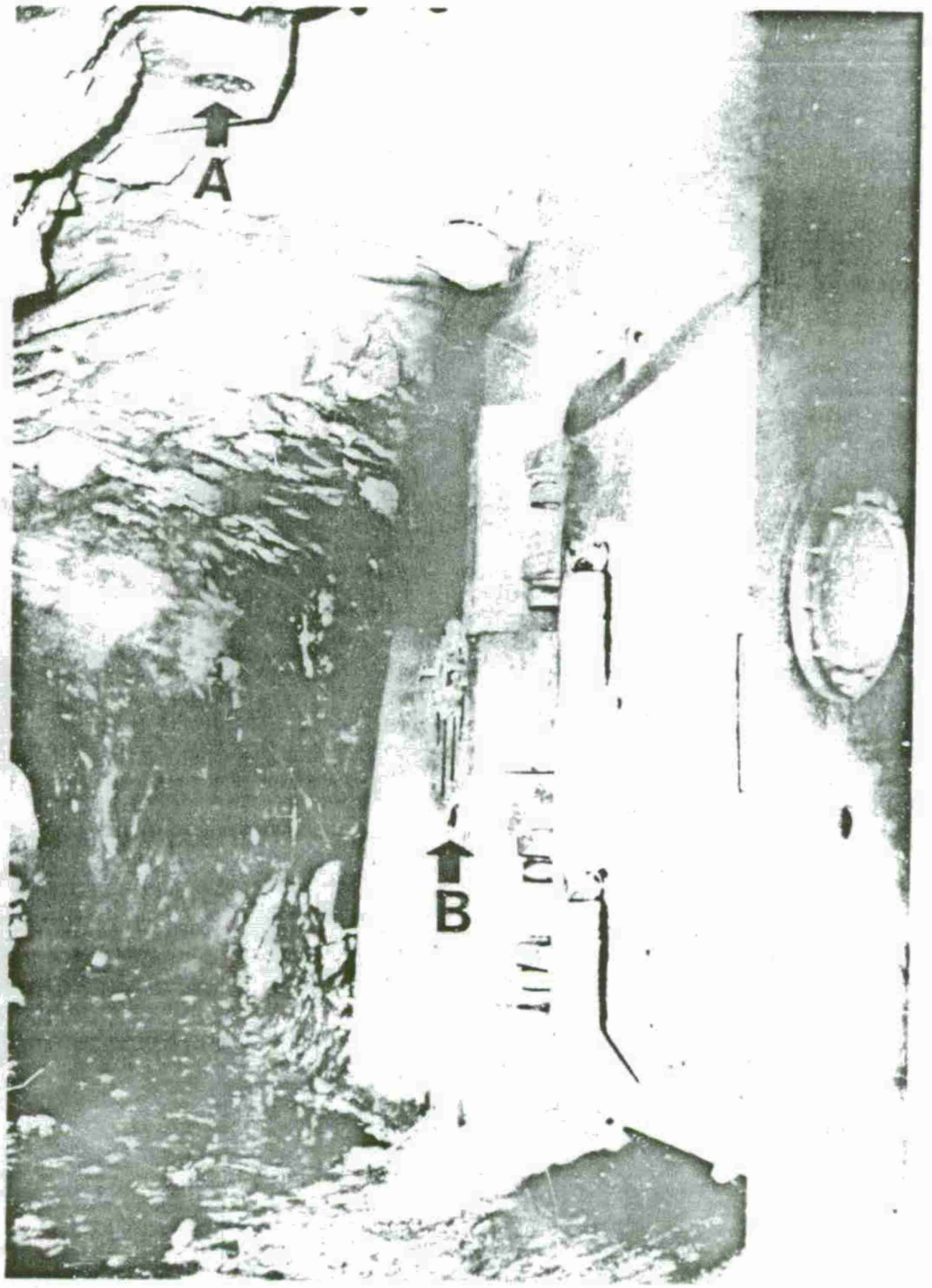

Figure 3.24 Measurement station 2 and 3

Note geometrical anomalies close to station 3 denoted by A. Station 2 is denoted by B.

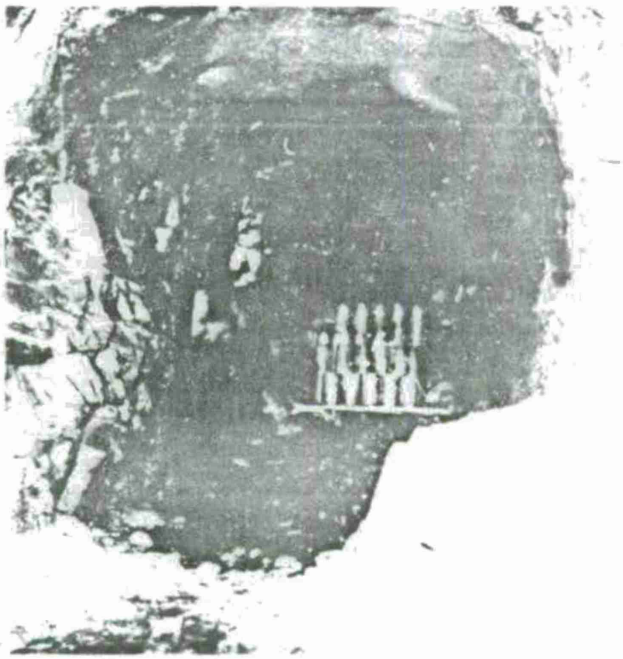

Figure 3.25 1000 kg TNT charge arranged in a stack close to the end wall in the tunnel, shot 8

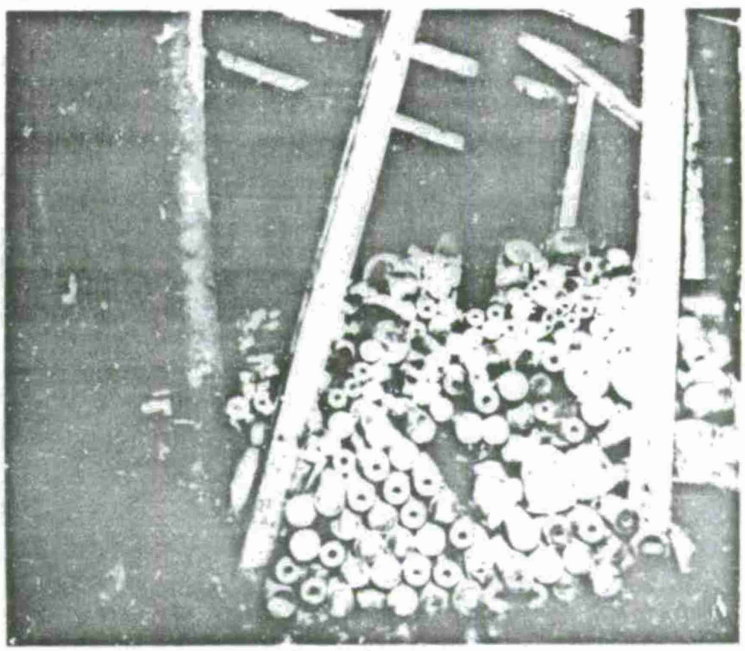

Figure 3.26 5400 kg TNT arranged for the final shot and partly shown on the picture

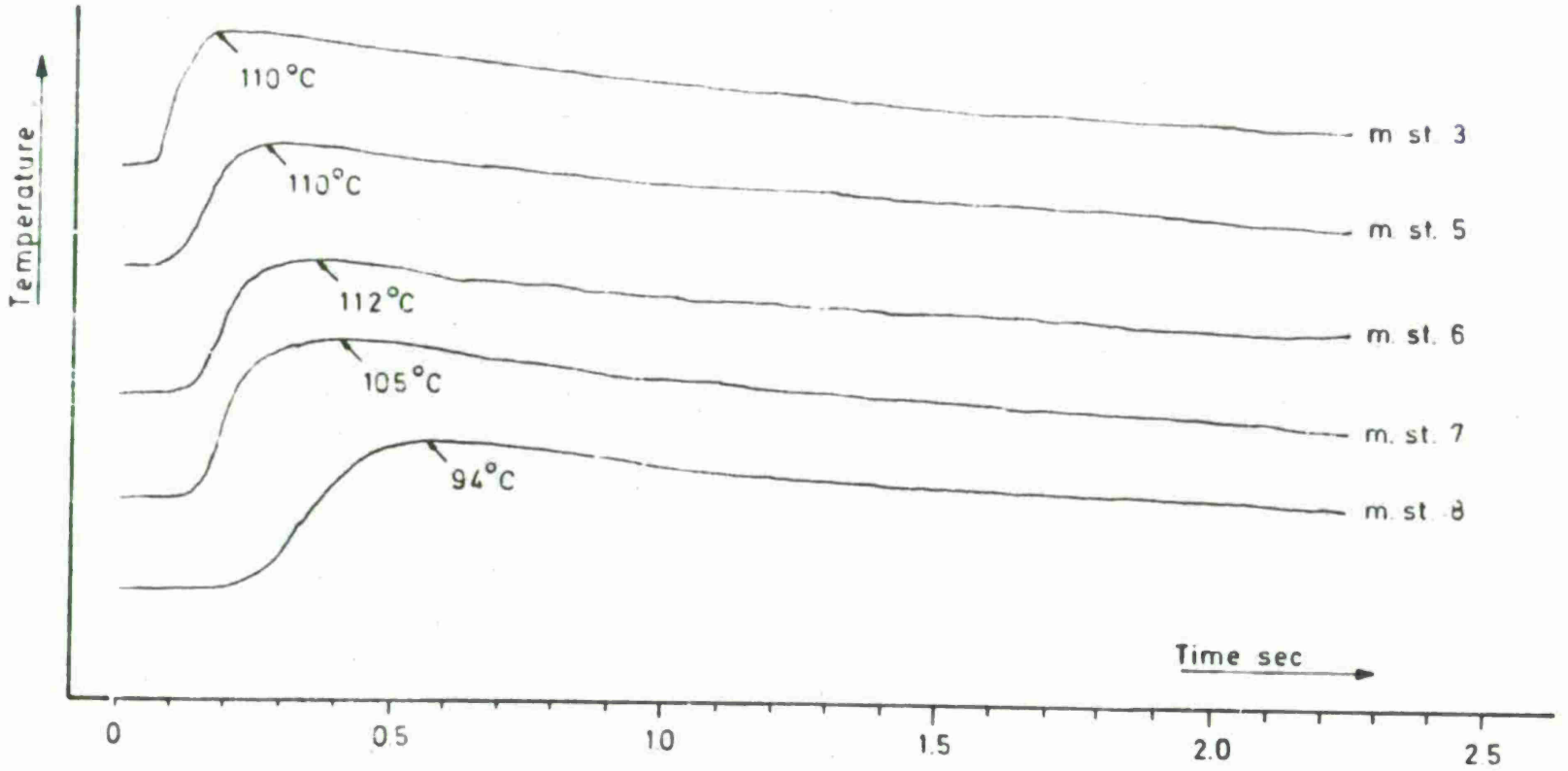

Fig. 3.27 Example of temperature records, shot 7